FOOD AND ECOLOGICAL SYSTEMS MODELLING JOURNAL

Food and Ecological Systems Modelling Journal 6: e152847 (2025)
DOI: https://doi.org/10.3897/fmj.6.152847

Formal Model Article Format

The Formal Model for the hoverfly *Eristalis tenax* (Diptera, Syrphidae) agent-based model in the Animal Landscape and Man Simulation System (ALMaSS)

Elżbieta Ziółkowska[1,2,3], Aleksandra Walczyńska[2], Christopher John Topping[1]

1 *Social-Ecological Systems Simulation centre, Department of Agroecology, Aarhus University, Aarhus, Denmark*
2 *Institute of Environmental Sciences, Faculty of Biology, Jagiellonian University, Kraków, Poland*
3 *Institute of Geography and Spatial Management, Faculty of Geography and Geology, Jagiellonian University, Kraków, Poland*
Corresponding author: Elżbieta Ziółkowska (e.ziolkowska@uj.edu.pl)

Abstract

We present a formal model for *Eristalis tenax*, the common drone fly, one of the most widespread syrphid species globally. This model is intended for inclusion in the Animal Landscape and Man Simulation System as a basis for regulatory assessment of the effects of pesticides on hoverfly pollinators. We propose to implement the model using an individual-based approach. The main drivers of the model are temperature, larval habitat distribution and quality, and nectar and pollen food resources in space and time. A prototype model description is presented that describes the full model, ready for implementation. The model considers individuals at all life stages, from egg to adult, with development from egg to pupa driven by temperature and larval development also influenced by larval density linked with the larval habitat quality. The model uses thermal performance curve models to represent the development and survival of the pupal stage, which is the most critical moment in the life cycle. Movement is modelled in detail, integrating dispersal, oviposition and foraging. Sources of mortality include overwintering mortality, slow development, density-dependent mortality at the larval stage, background mortality and pesticide and farm management mortality. A simple toxicological model is described as a basis for future expansion.

Key words: Agroecosystem, common drone fly, pollinators, population dynamics, spatially explicit model, syrphids

Academic editor: Fabio Sgolastra
Received: 13 March 2025
Accepted: 17 June 2025
Published: 18 July 2025

Citation: Ziółkowska E, Walczyńska A, Topping CJ (2025) The Formal Model for the hoverfly *Eristalis tenax* (Diptera, Syrphidae) agent-based model in the Animal Landscape and Man Simulation System (ALMaSS). Food and Ecological Systems Modelling Journal 6: e152847. https://doi.org/10.3897/fmj.6.152847

Introduction

Hoverflies, with more than 6000 species worldwide, are among the most important wild generalist pollinator groups, along with bees and bumblebees (Doyle et al. 2020). Although all hoverflies share the same indirect life cycle stages (egg, larva, pupa and adult), they can be distinguished by various larval feeding type (phytophagous, mycophagous, zoophagous and aquatic and terrestrial saprophagous species). Larvae of the genus *Eristalis* are aquatic and saprophagous, i.e. they filter feed on microbes in decaying organic matter and breathe using an elongated anal segment as a respiratory tube (Rotheray

1993), and can, therefore, potentially be used to degrade manure and other bio-organic wastes (Čičková et al. 2012; Van Huis 2013). For this reason, *Eristalis* species are often found in manure-polluted waters around farms in intensively managed agroecosystems.

Here, we present a Formal Model of a spatially-explicit agent-based model for the dronefly *Eristalis tenax* (Linnaeus, 1758) (Diptera, Syrphidae). The description follows the "Formal Model" format proposed by Topping et al. (2022) and is the first step in the model cycle before its implementation and calibration. The model is under development within the Animal, Landscape and Man Simulation System (ALMaSS) modelling framework (Topping et al. 2003; Topping 2022; Topping and Duan 2024a, 2024b). Therefore, we rely on this system"s features and adapt to the functional limitations imposed by the framework.

There are several existing or under-development individual-based models of hoverfly population dynamics, all focusing on aphidophagous hoverflies. These include the RePast hoverfly-aphid model described by Parry and Bithell (2011), the "Hover-Winter" model by Arrignon et al. (2007) which focuses on the overwintering population dynamics of *E. balteatus*, and the SyrFitSources spatially-explicit model of *E. balteatus* (App et al. 2025). However, to our knowledge, our model of *E. tenax* is the first spatially explicit individual-based model of a saprophagous hoverfly, linked with a detailed landscape model that provides a spatio-temporal assessment of food and habitat resources.

We selected *E. tenax* for modelling because it is a well-studied, synanthropic species that is widespread in temperate and continental climates around the world (in Europe, Asia, the Americas and Oceania; Francuski et al. 2014; Sengupta et al. 2016; Howlett and Gee 2019; Harris-Cypher et al. 2023). Adult drone flies are generalist pollinators, feeding on both pollen and nectar, visiting a wide range of flower colours and sizes (both wild and cultivated), with a preference for yellow flowers (An et al. 2018; Matoušková et al. 2023). *E. tenax* has been investigated as a potential managed crop pollinator, which could provide additional pollination services to bees (Howlett and Gee 2019). Protocols for laboratory rearing and long-term maintenance of *E. tenax* for research studies have been developed (Nicholas et al. 2018), as have attempts to create commercial mass-rearing systems (Upchurch et al. 2023), not only for commercial pollination but also for biodegradation in liquid and semi-solid environments (Hurtado 2013).

Aims and Purpose

The *E. tenax* model is designed to provide a realistic and detailed representation of hoverfly pollinators with aquatic and saprophagous larvae in European agricultural landscapes. The initial application of the model is to provide a representative of this group for use in a systems-based approach to regulators risk amendment for pollinators impacted directly or indirectly by agrochemical use, primarily by pesticides. As such, we have a specific section in the formal model for the implementation of exposure and effects of pesticides. The model will be developed in the ALMaSS framework at spatial scales of typically 100, but up to 2500 km^2, with a resolution of 1 m^2, and at daily time steps.

Theoretical framework and modelling approach

As with other published pollinator models in ALMaSS (Duan et al. 2022; Ziółkowska et al. 2023), we use an agent-based modelling approach (Grimm and Railsback 2005). Each hoverfly is represented as a separate object of a particular state with given properties, such as age, location and pesticide loading.

Our model is spatially explicit; thus, the position of each individual hoverfly (object) within a landscape is simulated. The ALMaSS modelling environment provides a detailed spatio-temporal representation of the landscape from which individual hoverflies obtain the information necessary to simulate their behaviour. This representation describes spatial landscape heterogeneity through a detailed raster land-cover map with a spatial resolution of 1 m^2. Farmed areas are represented as accurate maps of fields grouped into farm units of different types (e.g. cattle or arable farms). The temporal component of agricultural landscape heterogeneity refers to year-round crop management, described through individually tailored management plans for each crop. The cropping system is understood as a pluri-annual crop rotation. Crop management plans consist of combinations of farm activities (including pesticide treatments), time windows and probabilities of carrying out these activities. The temporal component includes weather conditions and vegetation growth models for all modelled vegetation types and crops; this is all updated daily. Such an approach gives a highly realistic dynamic landscape simulation with vegetation growing in response to the weather and the pattern of farming activities related to each crop, farm and field (Topping et al. 2016). The resource-providing units are the vital elements of the landscape simulation for all pollinators simulated within ALMaSS. These define the quantity and quality of pollen and nectar for each habitat patch in the landscape.

The model will consider the behaviour of all hoverfly life stages daily. The model"s parameters are based on the field and laboratory data on *E. tenax* available in the literature. When the necessary data were not available for *E. tenax*, we estimated parameters based on published data from other hoverfly species with similar life histories, particularly other species from the *Eristalis* genus, such as *Eristalis pertinax* (Scopoli, 1763) (similar size species found in Europe and Asia) and *Eristalis arbustorum* (Linnaeus, 1758) (the European drone fly of smaller size, abundant in Northern Hemisphere). The internal development of *E. tenax* individuals and interactions with each other and the environment are covered in each section below.

Framing the model

This section mentions some of the key problems and assumptions associated with the design of this model, and its linkage within the social-ecological systems and simulations where it will be used. The model aims to describe population changes in time and space and does not include all possible known behaviours unless these significantly influence population changes, with the aim to balance false inclusions and exclusions (Topping et al. 2015). Key assumptions are noted here, but for details see the discussion or details of the individual processes below.

The *E. tenax* model is built on extensive literature, though many processes have uncertain parameters and mechanisms, primarily derived from laboratory studies and other hoverfly species. Key assumptions and simplifications include:

- **Thermal Performance**: There is limited data for developmental stages, with a narrow temperature range tested, leading to potential biases in thermal performance curves.
- **Developmental Stages**: Simplified models for egg and larval stages are used due to insufficient data, with calibration needed for thermal limits.
- **Survival Data**: There is sparse data on juvenile survival, with suboptimal thermal performance curves for the pupa stage. Other mortality drivers are known but not well quantified.
- **Diet and Behaviour**: Hypotheses are based on related species for the diet (pollen to nectar ratio in daily diet depending on the ovarial development), assuming equal nutrient value from all pollen and nectar sources.
- **Energetic Budget**: No simulation of the energetic budget and gut filling is tracked separately for pollen and nectar.
- **Reproduction Parameters**: Variability in reproduction is poorly understood, with assumptions made based on laboratory conditions and other insect species.
- **Larval Habitats:** Use of a larval habitat quality index, with assumptions about density variation.
- **Dispersal**: Limited knowledge on the proportion of the population migrating. The probability of exhibiting migratory behaviour set as a fitted parameter which, for the sake of simplicity, is assumed to be zero in the first version of the model.
- **Phenology**: We assume that the phenology is parameterised for northern and central Europe, forcing a diapause situation in part of the population, which may not occur further south.
- **Density dependence**: We assume that density dependence works through two mechanisms: the availability of larval habitats and the larval density.

Other decisions are made primarily as a consequence of the available data in the supporting ALMaSS landscape framework (Topping and Duan 2024a). These include simplifications regarding the prediction of soil moisture and its calculation at the patch level and the fact that population genetics and behaviour related to genetic makeup are not considered, even though they may affect population processes in the long term. This is a consequence of an important simplification for efficiency: we assume that females can be mated and do not model males individually.

In this formal model, we have defined a simple toxicological model. This description is intended as a starting point only for future carefully developed toxicological models for regulatory use. Future versions may include expanding the current model to include sub-lethal effects and more detailed internal toxicology, such as implementing toxicokinetic/toxicodynamic models. The form that these models take will depend on the regulatory scenarios developed and, in particular, the design of exposure, which will be affected by the limitations in mapping larval habitats.

Framing the *E. tenax* model within the social-ecological systems it is a part of is largely a function of the ALMaSS landscape model and the scenarios designed for the model use. Key elements of this are related to the assumptions

regarding mapping details, pollen and nectar modelling, and human management, particularly farming. A discussion of these is outside the scope of this formal model. The main exclusion of those drivers that might change the model within the scope is the potential for different genetic traits and evolution. This omission is particularly important if local adaptation can alter key mechanisms represented in the model. However, including genetics will always be problematic due to the potential for seasonal long-distance dispersal.

Overview of processes

The common drone fly *E. tenax* is one of the most widespread syrphid species in the world. Due to its highly synanthropic nature, the species is found on all continents except Antarctica. Still, it is not common in extremely southern latitudes outside the arid areas of Europe, Asia, and Africa. It is especially abundant near human activity centres (Speight 2018). It is a large hoverfly with the mean mass of females around 140–150 mg, and males around 110–120 mg (Table 1). The colour patterns of this species are a clear example of Batesian mimicry with *Apis mellifera*. *Eristalis* spp. do not only mimic honeybees visually but also behaviourally during flight and feeding; they also produce a similar buzzing sound. *E. tenax*, or the drone fly, as its name suggests, is similar in appearance to male honey bees (drones) (Heal 1982; Bressin 1999; Golding and Edmunds 2000).

In northern and central Europe, *E. tenax* exhibits partial migratory behaviour, characterised by both seasonal migration and overwintering strategies. The expression of migratory activity is modulated by climatic variables, the spatial-temporal availability of resources and reproductive strategy imperatives (Tomlison and Menz 2015; Reynolds et al. 2024). The species is not found active in the field from around October/November to February/March, depending on the region (Kendall and Stradling 1972; Bressin 1999). As hibernation is mainly controlled by temperature and photoperiod, it starts earlier and ends later in colder regions further north compared to warmer regions in southern Europe. However, in Mediterranean climates, hoverflies can be found throughout the year (Pérez-Bañón et al. 2013), but the number of active hoverflies is much lower in winter.

Table 1. Data of *Eristalis tenax* mass (in mg) at each developmental stage, according to the collected literature. F – female, M – male; field – individuals collected in the field, lab – individuals emerged and reared in the laboratory conditions. No data was available for the larva stage. *Information provided to the authors by Francis Gilbert; sex unspecified.

Egg	Pupa	Adult	Reference
		F: 144.3 (75-211) M: 108.6 (63–176)	Bressin (1999)
0.184 (0.180-0.189)			Hurtado (2013)
	F: 180.2 M: 170.5	F: 99.6 M: 90.1	Ludoški et al. (2023)
		F (field): 149 (109-187) F (lab): 155 (103-191) M (lab): 122 (94-150)	Nicholas et al. (2018)
		110.2*	Wotton et al. (2019)
	249 (+/- 4.9)		Basley et al. (2018)
		F (field): 144.8 (+/- 5.94) M (field): 88.1 (+/- 9.06)	Tomlison and Menz (2015)

The development of the dronefly can be categorised into four main life stages: egg, larva, pupa, and adult. In central and northern Europe, there are usually two generations, spring/summer and autumn. A spring/summer generation begins in early spring with the emergence of females that were inseminated in the autumn, but the eggs did not develop until spring (Gilbert 1986; Bressin 1999; Upchurch et al. 2023). When the eggs are ready to be laid, a female searches for a suitable habitat for the larvae: stagnant water of various types (Campan and Campan 1979). The larvae, a type called a "rat-tailed maggot", are saprophagous and filter-feed on microbes associated with decomposing organic material, using a siphon (the "tail") to breathe (Kamdem and Otomo 2023). For pupation, the larvae crawl to a drier area and form a capsule to protect them from the environment during metamorphosis. The adults of the spring/summer generation mate and produce the autumn generation, which is much more abundant. As winter approaches, they begin to seek out moist crevices in rocks or buildings to hibernate (Bressin 1999). More details about each developmental stage are given below.

Growth and development

Egg

E. tenax eggs weigh around 180–189 µg (Table 1) and are laid side by side, perpendicular to the ground, in clusters, near or on the surface of stagnant water such as reservoirs, liquid manure or sewage. The duration of the egg phase is affected by temperature and humidity (Bressin 1999), but it is usually very short (2–3 days; Hartley 1961; Heal 1979; Gladis 1994; Basley et al. 2018; Campoy et al. 2020), mostly synchronised within one cluster. Egg cluster viability is rather high, estimated to be 86–100% by Bressin (1999).

Data on temperature-dependent development time at the egg stage were derived from five publications (Table 2). In Upchurch et al. (2023), the test was carried out at six temperatures, and unpublished data from Kendall (1971) are available for five temperatures, while in the other three studies, only one temperature ("room temperature") was used. The data collected follows a quadratic relationship (Equation 1), as shown in Fig. 1, but there was not enough data to estimate the thermal performance curve for egg development.

$$D_{egg}(T) = 0.025 \times T^2 - 1.421 \times T + 20.579 \quad \text{Equation 1}$$

where $D_{egg}(T)$ is the developmental time of the egg stage, and T is temperature.

Larva

The larva is saprophagous, called a rat-tailed maggot and is typical for syrphids, with a characteristic telescoping siphon that helps the larva breathe in its oxygen-deprived, organic-rich habitat. There are three subsequent larval stages in development, divided by moulting periods. Very high mortality at the beginning of the first instar larva stage is caused by difficulty in finding a suitable part of the habitat (Hartley 1961; Campoy et al. 2020). Another critical moment within a life cycle is the end of the third larval instar (Campoy et al. 2020). During this phase, the larva changes habitat to find a drier place, more suitable for pupation and metamorphosis.

Table 2. Summary of thermally induced length of development of subsequent life stages of *Eristalis tenax*. * Data from Kendall (1971), unpublished, were received via personal communication with Francis Gilbert.

Stage	Length (days)	Temperature (°C)	Reference
Eggs	4	12	Upchurch et al. (2023)
	2.8	16.5	
	1.8	21.5	
	2	24	
	1.4	25.5	
	1.2	30	
	1.5	20-25 (room temperature)	Dolley et al. (1933)
	2	Room temperature	Gladis (1994)
	2	25	Campoy et al. (2020)
	9	8	Kendall (1971) unpublished*
	12.8		
	8.8	12	
	10		
	2	21	
	2.8		
	1.9	22	
	2		
	2.9		
	1.8	24	
	2.6		
Larvae	28	20 (different densities and different experiments)	Hurtado (2013)
	30		
	32		
	28		
	29		
	33		
	19		
	25		
	31		
	16	19 (different diets)	Kamdem and Otomo (2023)
	16		
	21		
	14		
	15		
	17		
	11.3	21	Basley et al. (2018)
	14	22	Dolley et al. (1933)
	14	25	Campoy et al. (2020)
	86	8	Kendall (1971) unpublished*
	55	12	
	16	22-24	
	20		
	22		
Pupa	8-10	25	Perez-Banon et al. (2013)
	7	25 (different colouration of broods)	Heal (1989)
	8		
	8		
	7		
	7		
	30-44	10-12	
	17	17	
	25	15	
	47	10 (different colouration of broods)	
	36		

Stage	Length (days)	Temperature (°C)	Reference
Pupa	52	9 (different colouration of broods)	
	49		
	12	18	
	27	14 (different colouration of broods)	
	27		
	25		
	12	19	
	17	16	
	7	26	
	29	13	
	12	20 (different densities and different experiments)	Hurtado (2013)
	12		
	13		
	14		
	14		
	14		
	9		
	8		
	8		
	6	19 (different diets)	Kamdem and Otomo (2023)
	9		
	7	25	Campoy et al. (2020)
	7-8	22	Ludoški et al. (2023)
	8	22	Dolley et al. (1933)
	54	10	Daňková et al. (2023)
	26	12	
	14	17	
	11	23	
	8	25	
	44	8	Kendall (1971) unpublished*
	52		
	55		
	28	12	
	33		
	37		
	39		
	41		
	44		
	11	22-24	
	13		
	14		

The larva crawls using the pseudopodia (Buckton 1895) even several metres to find an optimal place for pupation (Hurtado 2013), and this movement can be quite rapid (>1 m/min) (Wilson et al. 2009). Larval development in *E. tenax* is temperature-dependent (Ottenheim et al. 1996; Hurtado 2013). It can also be impacted by the larval density and habitat quality, i.e., under nutritional stress, the larval developmental time increases (Equation 2), and the survival decreases (Equation 3) (Hurtado 2013; Fig. 2). These relationships may be described by linear functions:

$$D_{larva}(L_d) = 0.158 \times L_d + 15.673 \quad \text{Equation 2}$$

$$S_{larva}(L_d) = -0.475 \times L_d + 74.350 \quad \text{Equation 3}$$

where D_{larva} is the developmental time of the larval stage, S_{larva} is the larval survival and L_d is density of larvae.

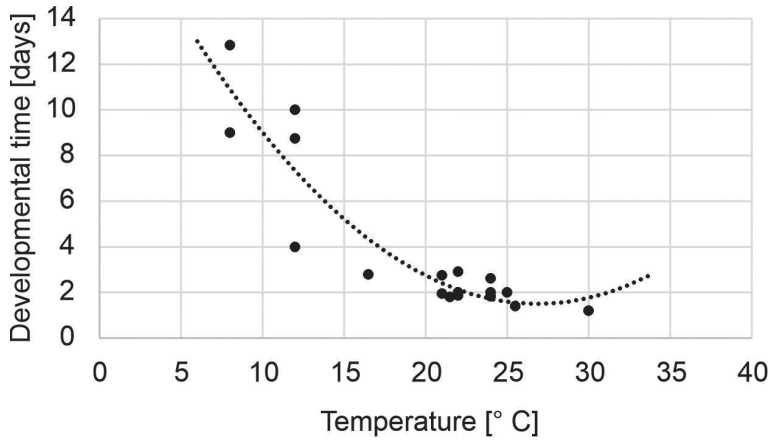

Figure 1. Relationship between temperature and egg development time of *Eristalis tenax* based on data from Table 2. Fitting quadratic equation to the data provides a model for egg developmental time and temperature (Equation 1; $R^2 = 0.85$).

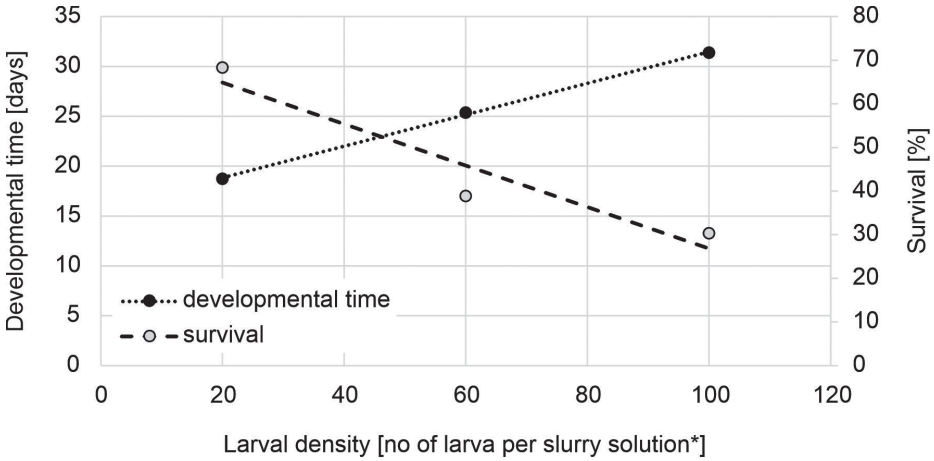

Figure 2. Dependence of *Eristalis tenax* larval developmental time and survival on larval density measured as number of larvae per slurry solution. Fitting linear equations to the data provides models for developmental time and larval density (Equation 2; $R^2 = 0.99$), and survival and larval density (Equation 3; $R^2 = 0.91$). Based on Hurtado (2013). * Slurry solution: 75 g of pig slurry mixed with 200 ml of water in 10.5 × 10.5 × 5 cm container of 0.5 l volume.

Density-dependent larval development in *Eristalis* species was earlier demonstrated by Kobayashi (1979), who investigated *Eristalis cerealis* (Fabricius, 1805) and found that, akin to *E. tenax*, larval development time in *E. cerealis* is prolonged under conditions of nutritional stress, accompanied by a concomitant decline in survival rates (Fig. 3). Furthermore, Kobayashi (1979) reported that nutritional limitations negatively affect larval biomass and body length in *E. cerealis* (Fig. 4).

Data on temperature-dependent larval development time (including stages 1–3) were derived from six publications (Table 2, Fig. 5). In two of them, larval development was tested in the normal thermal range, and additionally, it was tested either under different larval density conditions or food conditions. In three papers, only one temperature was used for the tests. Unpublished data from Kendall (1971) provide the only available information across a broader temperature range. The data collected follows a quadratic relationship (Equation 4), as shown in Fig. 5, but there was not enough data to estimate the thermal performance curve for larva development.

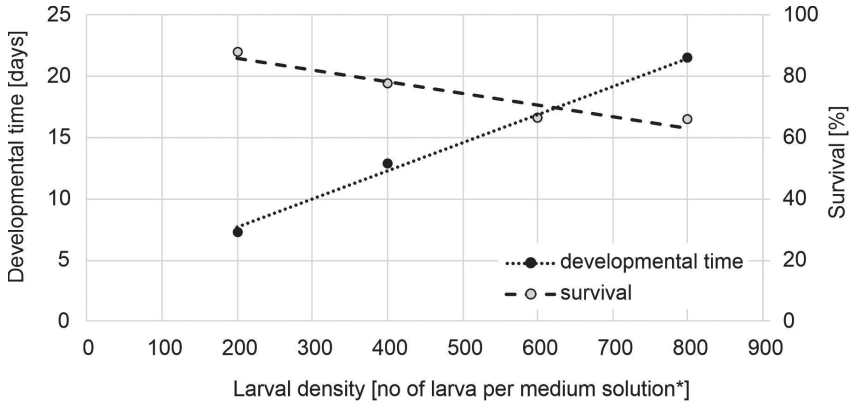

Figure 3. Dependence of *Eristalis cerealis* larval developmental time and survival on larval density measured as number of larvae per medium solution. Fitting linear equations to the data provides models for developmental time and larval density (R^2 = 0.99), and survival and larval density (R^2 = 0.91). Based on Kobayashi (1979). * Medium solution: Best among tested, barnyard-based diet provided in 20 × 30 × 5 cm container.

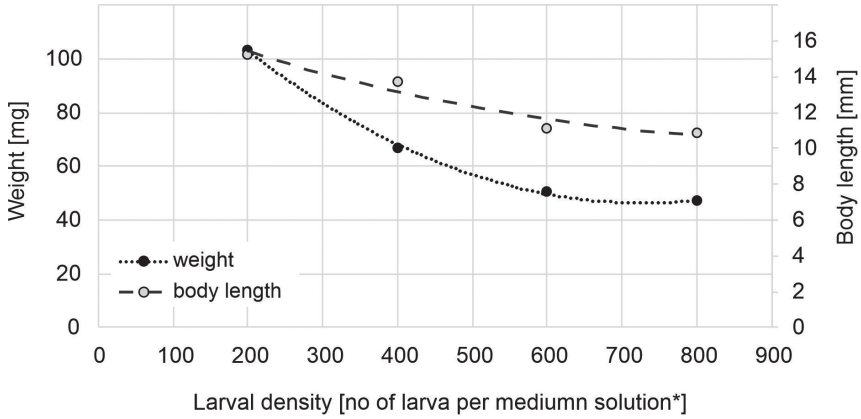

Figure 4. Dependence of *Eristalis cerealis* larval weight and body length on larval density measured as number of larvae per medium solution. Fitting quadratic equations to the data provides models for weight and larval density (R^2 = 0.99), and body length and larval density (R^2 = 0.95). Based on Kobayashi (1979). * Medium solution: Best among tested, barnyard-based diet provided in 20 × 30 × 5 cm container.

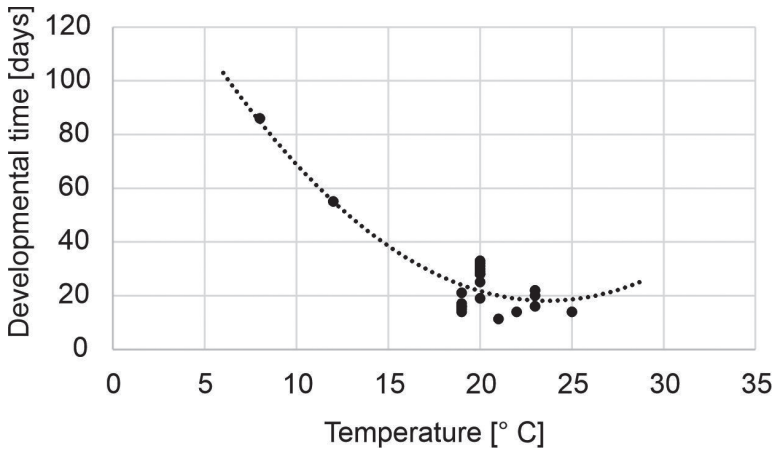

Figure 5. Relationship between temperature and larval development time of *Eristalis tenax* based on data from Table 2. Fitting quadratic equation to the data provides a model for larval developmental time and temperature (Equation 4; R^2 = 0.82).

Data on temperature-dependent larval development time is also available for a species of similar biology, *Eristales arbustorum* (Linnaeus, 1758), a European drone fly (Fig. 6; Ottenheim et al. 1996). *E. arbustorum* is a smaller hoverfly than *E. tenax* (9–11 mm length compared to 12–16 mm length of *E. tenax*). It appears to exhibit a shorter developmental duration at its thermal optimum (14 days versus 18 days) and a higher thermal optimum for development relative to *E. tenax* (27.0 °C versus 23.6 °C; according to Equations 4 and 6).

We found no data on the developmental time for individual instars for *E. tenax*. Such data is available for *Eristalinus arvorum* (Fabricius, 1787), an Asian hoverfly with saprophagous larva. *E. arvorum* is smaller than *E. tenax* (8–10 mm adult length compared to 12–16 mm adult length of *E. tenax*) and has a slightly shorter larval developmental time (11 days compared to 14 days at 25 °C for *E. tenax*) (Cao et al. 2022). The total larval developmental time for this species at 25 °C was divided into three instars: 31% for the 1st instar, 36% for the 2nd instar and 38% for the 3rd instar (Cao et al. 2022).

$$D_{larva}(T) = 0.272 \times T^2 - 12.886 \times T + 170.493 \quad \text{Equation 4}$$

$$D_{mlarva}(T) = 0.043 \times T^2 - 2.136 \times T + 40.680 \quad \text{Equation 5}$$

$$D_{flarva}(T) = 0.032 \times T^2 - 1.728 \times T + 37.361 \quad \text{Equation 6}$$

where D_{mlarva} and D_{flarva} is the developmental time of the larva stage for males and females, respectively, and T is temperature.

Pupa

The pupal weight is approximately 170–180 mg, with males being smaller than females (Table 1). It is an inactive stage, the duration of which depends on temperature. Some authors identify this stage as one of the most critical moments within the life cycle (Campoy et al. 2020), with mortality depending on temperature (Daňková et al. 2023). Two particularly vulnerable transitions within this stage include (1) the emergence of the pupal spiracles, a process that frequently fails and may compromise successful development, and (2) adult eclosion followed by wing expansion, which is also prone to failure (personal communication with F. Gilbert).

Temperature-dependent pupal development time data were derived from nine publications, four of which reported data from the wide thermal range (Table 2). Thermal performance curves for pupal development time were estimated using a set of models provided by the rTPC R package (Padfield et al. 2024) as described in Padfield et al. (2021). Such an estimation required the use of an inverse of development as the dependent variable. Table 3 shows the estimations of critical thermal minimum (CT_{min}), and critical thermal maximum (CT_{max}) across tested models. The graphical representation of the five best-performing models is shown in Fig. 7.

Planned implementation in the model

The model will consider *E. tenax* behaviour of all four life stages (i.e., egg, larva with three instars, pupa and adult) on a daily basis. We assume a ratio of 1:1 of females to males at the population level (following Ibrahim 1976, who investigated a large

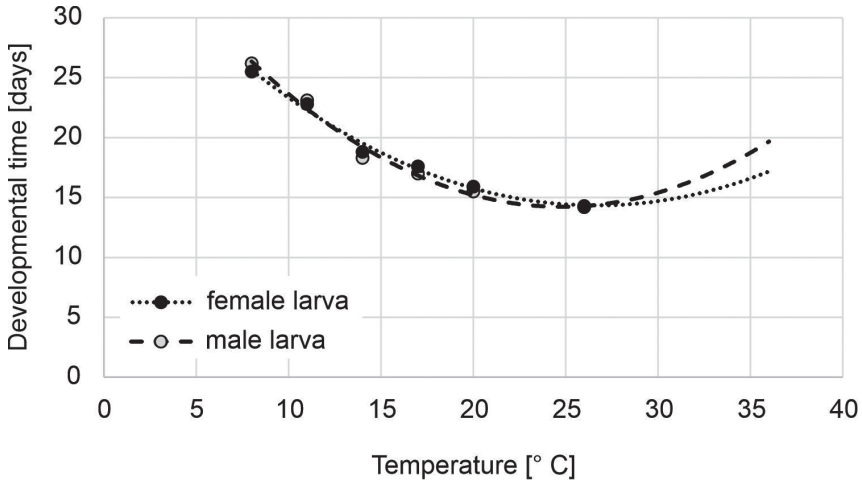

Figure 6. Relationship between temperature and larva development time of *Eristalis arbustorum* based on data from Ottenheim et al. (1996). *Eristalis arbustorum*, European drone fly, has a similar biology to *Eristalis tenax* although is smaller (9-11 mm length compared to 12-16 mm length of *Eristalis tenax*). Fitting a quadratic equation to the data provides models for developmental time and temperature, separately for males (Equation 5; $R^2 = 0.97$) and females (Equation 6; $R^2 = 0.99$).

Table 3. Parameters of the thermal performance curves fitted to the inverse of pupa developmental time for *Eristalis tenax*. CT_{Dpupa_min}, CT_{Dpupa_max} – critical thermal minima and maxima for the pupa stage. Model abbreviations follow convention used in rTPC R package (Padfield et al. 2024).

Model abbreviation	CT_{Dpupa_min}	CT_{Dpupa_max}
beta_2012	5.9	65.9
briere2_1999	4.6	40.8
delong_2017	5.0	53.8
flinn_1991	-10.6	60.6
gaussian_1987	5.5	46.5
hinshelwood_1947	20.1	58.4
joehnk_2008	4.6	32.4
kamykowski_1985	6.9	29.4
lrf_1991	6.4	31.6
modifiedgaussian_2006	4.8	47.2
oneill_1972	5.2	45.6
ratkowsky_1983	6.8	48.1
rezende_2019	0.1	31.5
thomas_2012	5.1	35.9
weibull_1995	5.2	41.7

field-sample of saprophagous hoverfly pupae of *Eristalinus taeniops* (Wiedemann, 1818) and thus, males will not be included in the model. It is further assumed that all adult females are fertilized; therefore, mating behaviour is not explicitly modelled, although it is implicitly incorporated into the timing of the reproductive process.

The development will be modelled according to the life-stage state machine and transition path (Fig. 8). Following emergence from hibernation in spring or arrival via migration, adult fertilised females begin interacting with their

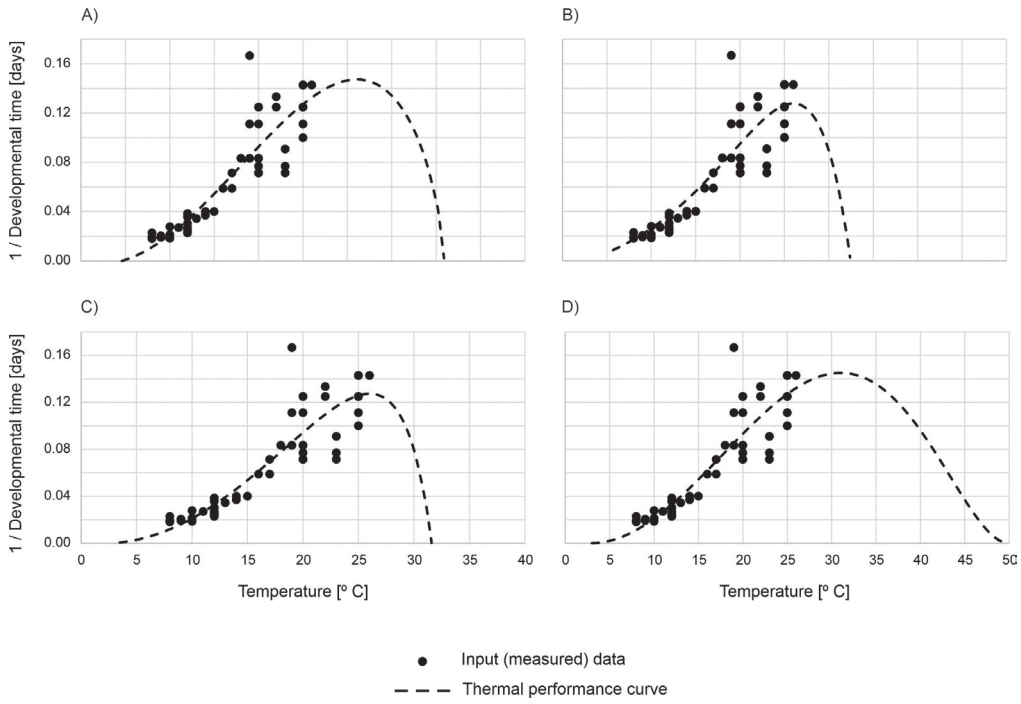

Figure 7. Relationship between temperature and pupa development time of *Eristalis tenax* according to four best-performing thermal performance curve models presented in Table 3: (A) briere2_1999, (B) joehnk_2008, (C) lrf_1991, and (D) ratkowsky_1983. The input (measured) data are presented as black dots. Performance of the models was similar with R^2 of 0.81 for briere2_1999, lrf_1991, and ratkowsky_1983 (0.81); and of 0.74 for joehnk_2008. Names of the thermal performance curves models after Padfield et al. (2024).

environment. This interaction includes dispersing in search of food resources, foraging for pollen and nectar, and reproducing (see section "Adults" for more details). Eggs are laid in clutches near a suitable habitat for the larvae, and their only behaviour is temperature-dependent development. The eggs hatch into larvae. On hatching, we assume that 50% are male and these are then removed from the model. Larval development occurs in stagnant water and depends on temperature and larval density (which is derived from larval habitat quality). The third larval instar crawls out onto dry land. We assume that this movement is rapid and takes place within one day. The length of the movement will be drawn from a uniform distribution with a maximum distance of D_l meters, and a minimum distance of 1 meter from the edge of the water body. As the exact movement capabilities of *E. tenax* larvae are not known, we assume D_l to be 10 m, subject to adjustment during the model calibration phase. The larvae transition into immobile pupae, and their development is temperature-dependent. The pupae eventually develop into adult females, forming the first, spring/summer generation. These spring/summer-generation adult females mate and produce a more abundant autumn generation, which subsequently hibernates. At each developmental stage, there is a probability of mortality (see section “Mortality”).

In the model, the temperature-dependent development on the egg stage will be modelled using a quadratic function (Equation 1) fitted to the data for *E. tenax* (Fig. 1) with an optimum at T_{opt} = 26.9 °C, at which the maximal developmental speed of 1.5 days is reached. Unfortunately, there was not enough data available to calculate the critical minimum (CT_{egg_min}) and maximum (CT_{egg_max}) temperatures for egg development. Thus, these values will be calibrated.

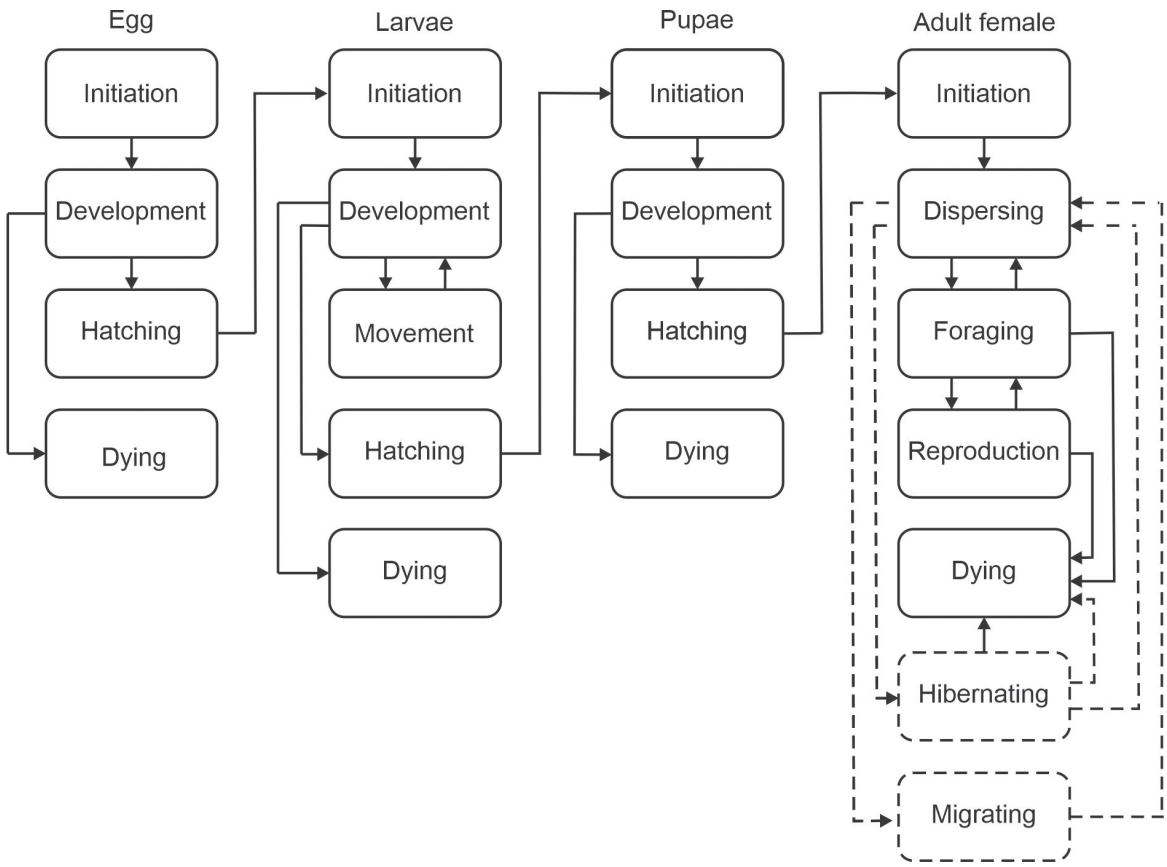

Figure 8. *Eristalis tenax* state diagram showing development from egg to adult female. All stages could transition to state Dying from any other behavioural state due to external messaging. The Hibernation and Migration states (dashed lines) only occurs for the second, autumn generation. It is assumed that a proportion of the population enters hibernation, while the remainder undertakes migration. Additionally, a subset of individuals may migrate into the landscape during the subsequent spring.

We will combine the dependence of larval development time on both temperature and larval density. The temperature dependence will be modelled using a quadratic function (Equation 4) fitted to the data for *E. tenax* (Fig. 5) with an optimum at T_{opt} = 23.6 °C, at which the maximal developmental speed of 18.1 days is reached. Unfortunately, there was not enough data available to calculate the critical minimum (C_{mlarva_min}) and maximum (CT_{larva_max}) temperatures for larval development. Thus, these values will be calibrated.

We will assume that the dependence on larval density (Fig. 2), which shows that larvae require more time to develop at higher larval densities, is valid for a temperature of 20 °C (as this was the constant temperature in the laboratory during Hurtado"s (2013) experiment). We will use a linear equation fitted to the three data points from Hurtado (2013) (i.e., development times measured for densities of 20, 60 and 100 larvae in a 10.5 × 10.5 × 5 cm container; Fig. 2) and a data point derived from the study of Ottenheim et al. (1996) by calculating the developmental time at 20 °C from Equation 5. In the study by Ottenheim et al. (1996), a maximum of 20 individuals of *E. arbustorum* were reared in 18 × 13 × 4.5 cm containers. As *E. tenax* is 1.3 times larger than *E. arbustorum* (12–16 mm length compared to 9–11 mm length of *E. arbustorum*), it can be assumed that the maximum larval density of *E. arbustorum* tested by Ottenheim et al. (1996) corresponds to 15.4 larval densities of *E. tenax*. Furthermore,

considering that the containers used for larval rearing in both studies by Hurtado (2013) and Ottenheim et al. (1996) were similar in terms of depth, and that *Eristalis* larvae stay close to the water surface to breathe, we can assume that the reported densities are related to the water surface area of the containers, i.e. 0.011 m^2 in the study by Hurtado (2013) and 0.0234 m^2 in the study by Ottenheim et al. (1996). We can then recalculate the densities reported in both studies to the number of larvae per m^2 of water surface and fit a linear equation relating larval density to development time at 20 °C (Equation 7).

$$D_{larva}(T = 20\ °C,\ L_d) = 0.002 \times L_d + 14.966 \quad \text{Equation 7}$$

where D_{larva} is the developmental time of the larval stage, L_d is larva density and T is temperature.

By linking Equation 4 and Equation 7, we will then create a family of quadratic curves (Fig. 9), parameterised so that their values reached at the temperature 20 °C match the larval density dependence (Equation 8).

$$D_{larva}(T,\ L_d) = 0.272 \times T^2 - 12.886 \times T + 0.002 \times L_d + 163.886 \quad \text{Equation 8}$$

In addition, an individual variation will be included around a maximal developmental speed (+/- 10%). The total developmental time for larvae will be divided into three instars using the proportions reported by Cao et al. (2022) for *E. arvorum*.

The duration of the pupal stage (inversion of developmental rate) will be related to the temperature using a thermal performance curve model of the Lobry–Rosso–Flandrois (LRF; lrf_1991). This model named by Ratkowsky and Reddy (2017) was proposed to represent microbial growth by Lobry et al. (1991) and Rosso et al. (1993). The four parameters in the model represent three cardinal temperatures (the maximum temperature at which development can occur T_{max}, the minimum development temperature T_{min}, and the optimum development temperature T_{opt}) and the specific growth rate at the optimum (U_{opt}). U_{opt} is independent of the three cardinal temperatures, and T is the temperature (Equation 9).

$$r(T) = u_{opt}\frac{(T - T_{max})(T - T_{min})^2}{(T_{opt} - T_{min})[(T_{opt} - T_{min})(T - T_{opt}) - (T_{opt} - T_{max})(T_{opt} + T_{min} - 2T)]} \quad \text{Equation 9}$$

Among similarly performing thermal performance curves we selected the LRF model as it was previously proposed to describe growth and temperature relationships in the agent-based model of another pollinator, the green-veined white butterfly *Pieris napi* (Topping and Duan 2025). After fitting the LRF model to our data, the parameters T_{min}, T_{opt}, T_{max} and U_{opt} were set to 2.16 °C, 26.00 °C, 31.59 °C and 0.13, respectively.

Adults

Diurnal activity

E. tenax is a strongly diurnal insect, with abundance varying throughout the day and tending to peak around midday, more or less coinciding with temperature and light (Bressin 1999; Thyselius 2022). Gilbert (1985a) also suggested a peak

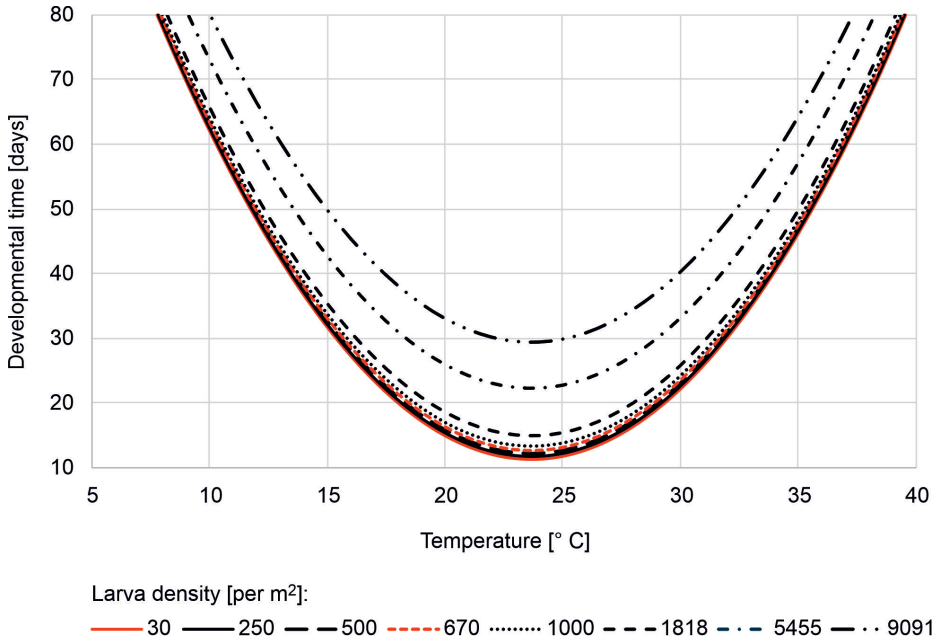

Figure 9. Dependence of *Eristalis tenax* larva developmental time on temperature and larva density. A family of quadratic curves for the developmental time is shown for larva densities from 30 to 9091 larvae per m^2 of water surface as presented in Table 4.

of feeding (on nectar) at around midday for *E. tenax*. It is possible that a trade-off has to be taken between the amount of nectar available and the energy needed to go and get it. Adult hoverfly activity appears to be driven by an internal circadian rhythm rather than external light. More detailed analyses showed that the activity of *E. tenax* males was influenced by time of day, but also by temperature and to some extent by light (the number of males increased with time and temperature, while light seemed to have a weak negative relationship with the number of flies), whereas the activity of females appeared to be influenced only by time of day (Bressin 1999). Thyselius (2022) showed that *E. tenax* activity remains robust in ageing hoverflies and found no difference in activity between females and males.

In the laboratory, hoverflies fly in the thermal range between 8 and 29 °C (Bressin 1999). Gilbert (1985a) reported that the lowest temperature at which *E. tenax* was observed was 10 °C, and the lowest temperature at which more than 50% of the flies were active was 11 °C. A similar temperature of 10 °C as critical for activity was also reported for male *E. tenax* in Canadian field studies (Wellington and Fitzpatrick 1981). According to the laboratory study by Kato (1943) (after Bressin 1999), certain ambient temperatures are required for *E. tenax* to become active: cleaning starts at 8 °C, crawling at 12 °C and normal activity at 15 °C. However, *E. tenax* has also been observed flying at lower temperatures of 4.5 °C in November and December in Japan (Kato 1943, after Bressin 1999), and at temperatures between 5–10 °C and under windy conditions (> 30 km/h) in New Zealand (Howlett et al. 2013). The observations may indicate that *E. tenax* is able to use solar radiation for temperature regulation (Bressin 1999). Flies tended to stop foraging and seek shade at temperatures above 30 °C (Jarlan et al. 1997). This is consistent with the findings of Kikuchi (1965) (after Bressin 1999). He observed that *E. tenax* appeared at ambient temperatures between 16 and 20 °C, reached maximum abundance at 25–28 °C and declined in numbers at temperatures above 28 °C.

Table 4. Developmental time of *Eristalis tenax* larva at 20 °C for larvae developing at different densities per m² of water surface. Relative density D_r is a density of larvae in a 10.5 × 10.5 × 5 cm container as used in the study of Hurtado (2013). Density L_d is a density per m² of water surface recalculated from relative densities assuming that $D = 0.011 \times D_r$. [1] Minimum and maximum densities of *Eristalis* species found in sewage settling ponds in Egypt from the study of Mahmoud (1997). [2] Minimum and maximum densities of *Eristalis* species found in sewage settling ponds in Egypt from the study of Ibrahim (1976). [3] Densities and developmental times at 20 °C corresponding to relative densities of 20, 60 and 100 used in the study of Hurtado (2013) are given for comparison.

Relative density (D_r)	Density (L_d) [m² of water surface]	Developmental time [at 20 °C]
0.3	30[1]	15.0
1.4	130[2]	15.2
2.8	250	15.4
5.5	500	15.9
7.4	650[1]	16.2
10.3	940[2]	16.7
11.0	1000	16.8
20.0[3]	1818	18.3
60.0[3]	5455	25.0
100.0[3]	9091	31.6

These observations are aligned with Campan"s (1968, 1973) findings that *E. tenax* exhibits a shift in diurnal activity rhythm in response to elevated temperatures. Specifically, as ambient temperatures increase, the species reduces its overall activity, resulting in a transition from a unimodal to a bimodal activity pattern. In Campan"s (1968) study, under low-to-moderate temperature conditions (14–25 °C), *E. tenax* visits to manure followed an unimodal distribution, with peak activity aligning closely with the daily thermal maximum. However, at higher temperatures (26–37 °C), the activity pattern became bimodal: the first peak occurred earlier in the day, before the thermal maximum, while the second peak occurred after the hottest period. Campan (1973) also observed that seasonal temperature fluctuations affect the frequency of unimodal versus bimodal activity days throughout the year.

It was observed (Gilbert 1985a) that *E. tenax* spends 79.3% of the time feeding, 13.1% resting and 0.6% flying, and that female hoverflies spent more time feeding than males.

Planned implementation in the model

We incorporate weather effects on hoverfly activity through an hourly weather assessment. Based on Gilbert (1985a), we assume that 50% of the population becomes active when the hourly daytime temperature reaches 11 °C, and 100% of the population is active when the temperature reaches 15 °C (as per Kato 1943, after Bressin 1999). This enables the calculation of the fraction of the population that is active (F_{activ}) at specific hourly temperatures (T_h) during the day, assuming a linear relationship (Equation 10).

$$F_{activ}(T_h) = 12.5 \times T_h - 87.5 \quad \text{Equation 10}$$

This activity is further restricted to daylight hours only (Fig. 10), and to specific rainfall and wind conditions (maximum acceptable rainfall R_{max} and wind speed W_{max} which will be calibrated). Individuals that become active at a given temperature are selected randomly from the population, reflecting the influence of varying local microclimatic conditions. From Equation 10 we can calculate the minimum temperature for activity to be 7 °C, which is consistent with the range of temperatures provided in the literature. In addition, after Jarlan et al. (1997), we will assume that the maximum temperature for activity is 30 °C.

Knowing when a given hoverfly starts and ends to be active during the day (based on temperature, rainfall and wind profiles during the day), we can calculate the total number of activity hours per day (h_{tot}). The total activity hours per day will then be divided into time spent on feeding (h_f), resting (h_r) and flying (h_m) based on proportions provided by Gilbert (1985a). These proportions were derived from instantaneous behavioural observations recorded at the moment of first sighting, with the aggregated data interpreted as representative of the species" energy budget. For the purposes of this study, we assume that "feeding" time includes all local movements within the flower patch, whereas "flying" time covers movements between flower patches. This would imply that there is a local movement distance threshold d_l (to be calibrated) above which a movement bout is considered to be long enough to allow a hoverfly reaching flight speed to find a new flower patch (see "Dispersal" for details). We further assume, after Thyselius (2022), that the activity pattern of *E. tenax* does not change with the hoverfly"s age.

Foraging

Gilbert (1985b) analysed dietary preferences (estimated feeding-time-budgets) of hoverflies based on field observations and categorised hoverflies according to the proportion of time spent feeding on nectar versus pollen. In this study, *E. tenax* was categorised as a mixed-feeder, feeding on both pollen and nectar. Hoverflies participate in pollination as a result of the pollen getting stuck to their hairs. When foraging, dipterans use visual cues for long distances and olfactory ones for short distances (Willmer 2011).

To our knowledge, there is only limited information on the energetics of *E. tenax* and other hoverflies. Existing studies focus on examining the diets of hoverflies by analysing dissection of their intestines or their excrements (which allows identification of the pollen types ingested; e.g. Halloway 1976; Irvin et al. 1999), pollen transport by hoverflies (Lucas et al. 2018), or impact of type of food consumed on hoverfly"s performance (i.e., longevity, activity or survival; i.e., Pinheiro et al. 2015; Thyselius and Nordström 2016). The only detailed analyses of energetics of the foraging behaviour of *E. tenax* was presented by Sotavalta and Laulajainen (1961) and Gilbert (1983). Gilbert (1983) found that the energy gain while foraging on *Aster* is low (0.01 W) and that when continuously foraging on *Aster* nectar, the hoverflies can fill their crop in about 75–220 min, assuming the average and maximal crop volumes of 5.8 and 17.2 µl respectively. Gilbert (1983) suggested that *E. tenax* can thus make a sizeable energetic profit, even at low nectar availabilities.

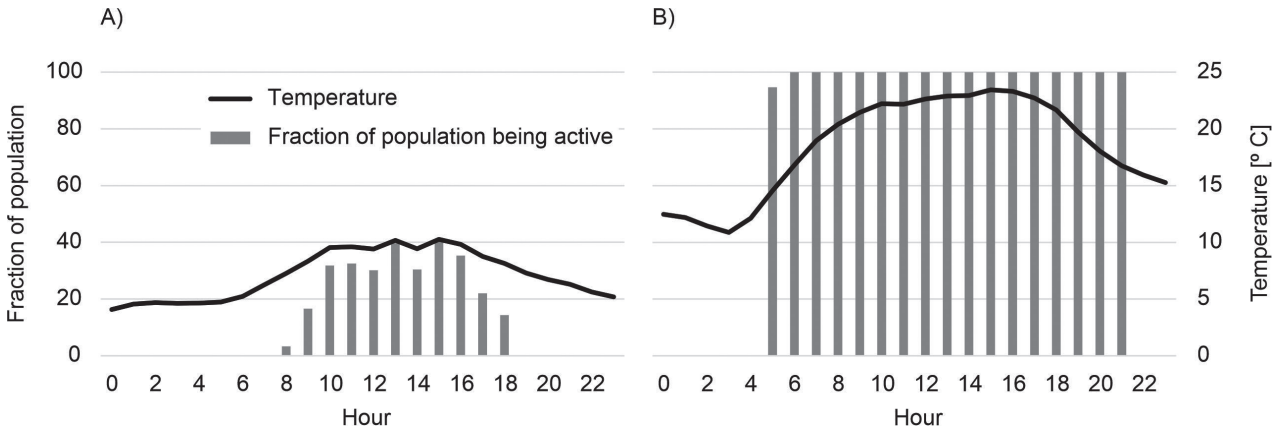

Figure 10. Fraction of hoverfly population being active on two selected days near Warsaw (Poland) in 2009, calculated based on Equation 10: (A) on March 27th, and (B) on June 27th. The activity is restricted by the temperature and photoperiod.

Food requirements

Both *E. tenax* males and females usually eat pollen at the beginning of their life because adults emerge with immature reproductive organs and gametes, and pollen proteins are essential for maturation (Gilbert 1986). Subsequently, females consume more pollen than nectar because it is needed for egg maturation (Gilbert 1985b). Males that hover have been found to have their abdomen partly filled with air, probably to reduce their mass and save energy, and tend to feed on nectar only (Gilbert 1986). These distinct food requirements between female and male hoverflies were confirmed by several studies on the gut content of hoverflies in which the amount of pollen was larger in the gut content of gravid females compared to non-gravid females and males (Haslett 1989; Irvin et al. 1999; Villa et al. 2021).

The detailed study of the gut contents in *Rhingia campestris* (Meigen, 1822) hoverfly (body length of 8–11 mm, wingspan of 12–18 mm) showed a relationship between diet and the degree of ovarian development in females. Females switch from nectar to pollen feeding during the maturation of ovaries and back to nectar feeding once eggs are laid (Haslett 1989; Fig. 11). For females, nectar-feeding is thus associated with mating and oviposition, activities that have substantial energy costs (Gilbert 1986). Based on personal observation, Haslett (1989) suggested that a similar pattern can be observed in other hoverfly species, including *E. tenax*.

Food preferences

E. tenax forage on a wide range of flowers. Flower choice is made according to the nutritional value of the pollen provided by the flower and according to the colour of the petals (Bressin 1999).

E. tenax exhibits distinct floral preferences influenced by the colour, size, and UV properties of flowers. Studies have shown that yellow is the most preferred colour for both landing and proboscis extension, with larger yellow flowers being particularly attractive (Matoušková et al. 2023). The preference for yellow is so strong that it triggers landing regardless of UV reflection, while proboscis extension is specifically triggered by yellow colours that absorb blue and UV light (Lunau and Wacht 1994; Lunau and Wacht 1997; An et al. 2018). Despite

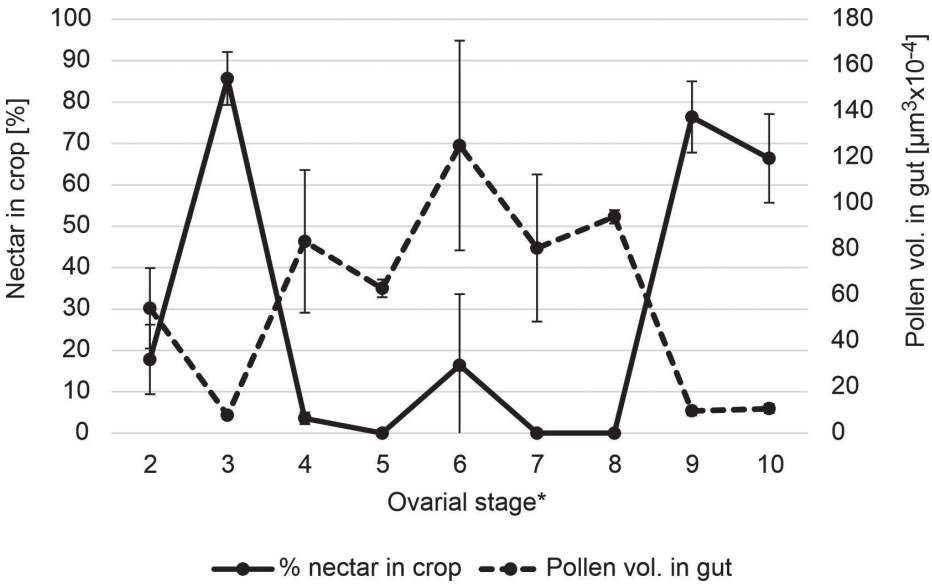

Figure 11. Relationship between ovarial development and diet of adult female hoverfly *Rhingia campestris*. Points are means from a minimum of 4 flies. Vertical lines represent standard error (based on Haslett 1989). *Ovarial stages considered: (1) the germarium, (2) the newly formed follicle, spherical in shape, the oocyte within is not visible, (3) the oocyte is distinct from the nurse cells within the slightly ovate follicle, but forms less than 10% of the total follicular volume, (4) the oocyte occupies between 10% and 20% of the follicle, which is now distinctly oval in shape, this stage represents the onset of yolk deposition, (5) the oocyte (with yolk) occupies 20%-30% of the follicle, (6) the oocyte occupies 30%-50% of the follicle, (7) the oocyte occupies 50%-75% of the follicle, (8) the oocyte occupies up to 90% of the follicle, yolk deposition is near completion, (9) the mature egg, occupying nearly the entire follicle, the egg is more opaque than at earlier stages and is longer and thinner, (10) the eggs have been discharged and the ovaries have shrunk and appear rather degenerate.

their ability to learn to land on other colours, *E. tenax* still shows a significant preference for yellow and UV-absorbing colours over UV-reflecting ones. Additionally, these flies tend to avoid dark colours, except for yellow, and prefer bright colours for landing (An et al. 2018). The spectral sensitivity of their proboscis reaction is finely tuned to a small range of wavelengths (520–600 nm), which aligns with the yellow colour of pollen and floral guides in natural flowers (Wacht et al. 1996). This innate preference for yellow and the limited ability to condition their proboscis reflex to other colours suggest that *E. tenax* has evolved specific perceptual dimensions for yellowness and blueness, optimizing their foraging efficiency on yellow flowers (An et al. 2018).

In the case of *E. tenax*, the plant-pollinator interactions were analysed using different methods: direct visual observations (Cowgill 1991; Hoffmann 2005; Klecka et al. 2018; Ouvrard et al. 2018; Plume et al. 2024), analysis of the gut content (Irvin et al. 1999), analysis of pollen carried by hoverflies on their body (e.g., Holloway 1976) or DNA metabarcoding (Lucas et al. 2018). Based on these publications, a summary of plants visited by *E. tenax* is presented in Table 5. The table does not distinguish between plants visited by female and male hoverflies, as according to Klecka et al. (2018) differences in flower preferences between sexes in *E. tenax* are negligible.

Table 5. Summary of plant species visited by *Eristalis tenax*.

Species	Genus	Family
Acer pseudoplatanus	*Acer*	Sapindaceae
Achillea millefolium	*Achillea*	Asteraceae
Aegopodium podagraria	*Aegopodium*	Apiaceae
Agrimonia eupatoria	*Agrimonia*	Rosaceae
Anethum graveolens	*Anethum*	Apiaceae
Anthriscus sylvestris	*Anthriscus*	Apiaceae
Ballota nigra	*Ballota*	Lamiaceae
Borago officinalis	*Borago*	Boraginaceae
Brassica type	*Brassica*	Brassicaceae
Buddleja type	*Buddleja*	Scrophulariaceae
Calendula arvensis	*Calendula*	Asteraceae
Calendula officinalis	*Calendula*	Asteraceae
Calluna vulgaris	*Calluna*	Ericaceae
Capsella bursa-pastoris	*Capsella*	Brassicaceae
Carum carvi	*Carum*	Apiaceae
Centaurea cyanus	*Centaurea*	Asteraceae
Centaurea jacea	*Centaurea*	Asteraceae
Centaurea nigra	*Centaurea*	Asteraceae
Centaurea scabiosa	*Centaurea*	Asteraceae
Cichorium intybus	*Cichorium*	Asteraceae
Cirsium arvense	*Cirsium*	Asteraceae
Cirsium palustre	*Cirsium*	Asteraceae
Clematis vitalba	*Clematis*	Ranunculaceae
Convolvulus arvensis	*Convolvulus*	Convolvulaceae
Crataegus monogyna	*Crataegus*	Rosaceae
Crepis capillaris	*Crepis*	Asteraceae
Daucus carota	*Daucus*	Apiaceae
Erica cinerea	*Erica*	Ericaceae
Erica tetralix	*Erica*	Ericaceae
Eupatorium cannabinum	*Eupatorium*	Asteraceae
Filipendula ulmaria	*Filipendula*	Rosaceae
Foeniculum vulgare	*Foeniculum*	Apiaceae
Galium type	*Galium*	Rubiaceae
Glebionis segetum	*Glebionis*	Asteraceae
Hedera helix	*Hedera*	Araliaceaes
Helianthemum nummularium	*Helianthemum*	Cistaceae
Heracleum sphondylium	*Heracleum*	Apiaceae
Hypericum perforatum	*Hypericum*	Hypericaceae
Hypochaeris radicata	*Hypochaeris*	Asteraceae
Juncus type	*Juncus*	Juncaceae
Hypochaeris radicata	*Hypochaeris*	Asteraceae
Knautia arvensis	*Knautia*	Dipsacaceae
Lapsana communis	*Lapsana*	Asteraceae
Lamium album	*Lamium*	Lamiaceae
Lamium purpureum	*Lamium*	Lamiaceae
Lavandula angustifolia	*Lavandula*	Lamiaceae

Species	Genus	Family
Leontodon autumnalis	*Leontodon*	Asteraceae
Leontodon hispidus	*Leontodon*	Asteraceae
Leontodon saxatilis	*Leontodon*	Asteraceae
Leucanthemum vulgare	*Leucanthemum*	Asteraceae
Ligustrum vulgare	*Ligustrum*	Oleaceae
Lonicera periclymenum	*Lonicera*	Caprifoliaceae
Lotus corniculatus	*Lotus*	Fabaceae
Lotus pedunculatus	*Lotus*	Fabaceae
Matricaria perforata	*Matricaria*	Asteraceae
Mentha aquatica	*Mentha*	Lamiaceae
Origanum vulgare	*Origanum*	Lamiaceae
Oxalis pes-caprae	*Oxalis*	Oxalidaceae
Pastinaca sativa	*Pastinaca*	Apiaceae
Persicaria amphibia	*Persicaria*	Polygonaceae
Pilosella officinarum	*Pilosella*	Asteraceae
Plantago lanceolata	*Plantago*	Plantaginaceae
Potentilla type	*Potentilla*	Rosaceae
Ranunculus acris	*Ranunculus*	Ranunculaceae
Ranunculus repens	*Ranunculus*	Ranunculaceae
Rubus fruticosus agg.	*Rubus*	Rosaceae
Scabiosa columbaria	*Scabiosa*	Dipsacaceae
Senecio jacobaea	*Senecio*	Asteraceae
Silene albescens	*Silene*	Caryophyllaceae
Silene dioica	*Silene*	Caryophyllaceae
Sinapis arvensis	*Sinapis*	Brassicaceae
Sonchus arvensis	*Sonchus*	Asteraceae
Sonchus asper	*Sonchus*	Asteraceae
Succisa pratensis	*Succisa*	Caprifoliaceae
Taraxacum officinale agg.	*Taraxacum*	Asteraceae
Thymus pulegioides	*Thymus*	Lamiaceae
Thymus vulgaris	*Thymus*	Lamiaceae
Trifolium pratense	*Trifolium*	Fabaceae
Trifolium repens	*Trifolium*	Fabaceae
Urtica dioica	*Urtica*	Urticaceae
Vicia cracca	*Vicia*	Fabaceae

Planned implementation in the model

Since the foraging movements are intertwined with reproduction and dispersal, we consider foraging movement under the heading "Dispersal" below.

Following Haslett (1989), we assume that a female hoverfly switches the ratio of pollen to nectar in her daily diet depending on her behavioural state, and that she can forage on pollen and nectar at the same time (from the same habitat patch if both resources are available). Thus, depending on the behavioural state, the female will have a specific foraging goal expressed in terms of the ratio of pollen to nectar. During ovarian development and egg maturation, the female will feed mainly on pollen (foraging goal 90:10 pollen to nectar ratio), whilst during mating and oviposition, the female will feed mainly on nectar (foraging goal 20:80 pollen to nectar ratio).

We further assume (following Gilbert 1983) that *E. tenax* can make a sizeable energetic gain even at low nectar availability, thus replenishing the energy lost during flight very quickly. Therefore, we do not intend to model the energetic budget of the hoverfly (linking energy losses with flying and mating activities and energy gains with nectar foraging). Instead, the percentage of gut filling will be tracked in the model separately for pollen and nectar resources (according to the foraging goals). We assume that the gut volume (G_v) corresponds to maximum crop volumes measured by Gilbert (1983), i.e., vary between 5.8 and 17.2 µl, depending on the hoverfly"s mass (M). Here, a linear relationship between gut volume and mass will be assumed (Equation 11), considering the mass range of females from 109 to 187 mg (as measured for hoverflies from the field; Nicholas et al. 2018).

$$G_v(M) = 0.13 \times M - 8.16 \quad \text{Equation 11}$$

We further assume that the hourly rate of food (pollen or nectar) intake r_h in hoverflies is limited and depends on the gut volume (i.e., it can be represented as a fraction of the gut volume). Knowing the number of daily foraging hours, we can calculate the maximum daily food intake (Equation 12) and, hence, the maximum fraction of the gut which can be filled within a day. Thus, by changing r_h, we can change the minimum time it takes for a hoverfly to reach its reproduction goals (see "Reproduction" for details).

$$F_{max} = r_h \times h_f \times G_v(m) \quad \text{Equation 12}$$

where F_{max} is the maximum daily food intake, h_f is the number of daily foraging hours, and r_h is the maximum hourly rate of food intake ($0 < r_h < 1$) to be calibrated.

The maximum daily food intake F_{max} will be a sum of pollen and nectar in a proportion in line with the current foraging goal. The amount of pollen and nectar needed to completely fill the gut, and thus the maximum daily food intake (F_{max}), will be calibrated to the amount of resources available in the environment, such that when resources are low, it is much more difficult to reach a full gut than when resources are high. This calibration will take into account the reproductive goals (see "Reproduction" below) as these are associated with certain levels of gut filling.

The amount of pollen and nectar available to *E. tenax* from each habitat patch in the landscape per day will be modelled in ALMaSS using the floral resource models. The floral resource models have been developed within the B-GOOD Horizon 2020 project (Ziółkowska et al., unpublished). The framework integrates data on the amount of pollen, nectar and sugars produced by a single flower/inflorescence of a given plant species with information on flower/inflorescence abundance (i.e. density of flowers/inflorescences per unit area), flowering phenology, plant composition of the habitat and habitat composition and configuration within the landscape. This approach makes it possible to predict the spatio-temporal availability of floral resources within different habitat types and across different landscapes.

The amount of pollen available to *E. tenax* in the landscape will be limited to those plants visited only by *E. tenax*. Such a list of plants will be available based on analysis of plant-pollinator interactions. Table 5 presents a preliminary list of plants visited by *E. tenax*, which could be further revised by additional literature searches and expert knowledge. In addition, the daily pollen attractiveness

P_h of a given habitat patch *h* will be calculated by multiplying the amount of pollen resources *P* available to *E. tenax* from each plant *p* in the patch on day *d* by the plant"s pollen preference score p_s (Equation 13). The amount of pollen resources produced by plant *p* on day *d* in habitat patch *h* results from the daily pollen production of the plant, the proportion of the plant in the habitat patch and the area of the habitat patch. The pollen preference score p_s of a plant is a pollinator-specific measure on a semi-quantitative scale (from 0 to 3), calculated on the basis of plant-pollen interactions and the nutritional and chemical properties of a pollen (i.e. protein to lipid ratio and potassium to sodium ratio). The pollen preference score p_s is being developed in the Better-B Horizon Europe project and will be linked to the floral resource models in ALMaSS.

$$P_h = \sum_p P_{p,d} \times p_s \quad \text{Equation 13}$$

The daily pollen attractiveness P_h of a given habitat patch *h* in a landscape will be further scaled by the nectar attractiveness N_h modified by a scalar *c* (to be calibrated) to obtain the daily food attractiveness F_h of the patch (Equation 14). To our knowledge, detailed information on the nectar preferences of *E. tenax*, particularly regarding sugar concentration preferences, is lacking. Gilbert (1981) investigated the ingestion rates of sugar solutions ranging from 10% to 67% in various hoverfly species, including *E. tenax*. While complete data were available for *Syrphus ribesii* (Linnaeus, 1758), indicating an optimal energy intake rate at approximately 50% sugar concentration, the data for *E. tenax* were incomplete. However, the available results suggest that *E. tenax* exhibits lower ingestion rates compared to *S. ribesii*, ranging from 0.31–0.35 µl/s for 20–30% solutions and declining to 0.04 µl/s at 67% concentration. Given the limited empirical data, we assume that the daily nectar attractiveness of a given patch *h* is proportional to the total daily nectar production of all plant species within that habitat that are visited by *E. tenax*. This assumption can be changed later when more information on *E. tenax* nectar preferences is available.

$$F_h = P_h \times N_h \times c \quad \text{Equation 14}$$

Reproduction and oviposition

E. tenax exhibits bivoltinism, producing two generations annually (Gilbert 1986; Bressin 1999; Upchurch et al. 2023). Although details on number of mating events are lacking for *E. tenax*, insights can be drawn from related species. For instance, Gladis (1993, 1994b) investigated the reproductive behaviour of *Helophilus pendulus* (Linnaeus, 1758), another hoverfly species with saprophagous larvae. The study demonstrated that females of *H. pendulus* are capable of multiple mating events. Under controlled laboratory conditions, individual females underwent up to three copulation-oviposition cycles. Following the third cycle, reproductive activity declined. While occasional copulation was still observed, it was not accompanied by complete egg development, suggesting a reduction in reproductive potential after successive mating cycles.

Mating can last from seconds to hours. Males hover and wait or search for passing females with which to mate. Several authors have reported that male hovering activity is timed to coincide with female activity, as it is energetically

demanding (Thyselius 2022). In *Eristalis* spp., the eggs are not immediately fertilized but are stored in the female spermathecae. The sperm are nourished by the secretions of the female"s special tube glands. These glands are particularly well developed in *E. tenax*, in which the sperm of the autumn (second) generation of females are nourished throughout the winter, and the eggs are not fertilized until the spring (Gilbert 1986). After hibernation, *E. tenax* females require a certain number of days for the development of their ovaries and maturation of eggs. This pre-oviposition period could vary considerably, from 10 to even 38 days, with a mean around 20 days (Table 9).

E. tenax lays eggs in clutches. The total reproductive potential (the total number of eggs) of a female, and the number and size of clutches differ considerably (Table 9). Honěk (1993) found a linear relationship between fecundity and adult female dry weight, and between number of ovarioles and adult female dry weight for oviparous insects, including Diptera. Although *E. tenax* was not covered in this study, data were included for another hoverfly, *Metasyrphus corollae* (Fabricius, 1794) (Scott and Barlow 1984). Gladis (1993, 1994b) identified a consistent pattern in the reproductive behaviour of *H. pendulus*. Females typically deposited eggs in two to three (or more) adjacent clutches on the same day, with occasional additional egg deposition occurring the following day. The initial oviposition generally took place approximately one week after mating. Subsequent mating events occurred immediately following oviposition, with intervals between mating and the next oviposition ranging from 10 to 14 days. In contrast, *E. tenax* exhibits more variable inter-oviposition intervals, ranging from 2 to 12 days (see Table 9). As egg maturation within the ovaries is a gradual process, these intervals allow the female to accumulate sufficient nutrients and energy reserves. At the population level, in the lab conditions, Upchurch et al. (2023) found that the peak of egg production in *E. tenax* occurs around the 5th (22% of total egg production) and 8th (20%) weeks of the hoverfly"s life. The variability in *E. tenax* reproduction parameters depends on various factors, including energy reserves, nutrient availability and environmental factors (Gladis 1994).

During oviposition, *E. tenax* females are attracted by the odour of manure, stagnant water, decaying matter, etc. (Bressin 1999). On farms, females can lay eggs in cracks in the walls of septic tanks and even on the dry crust of slurry. Studies of larval densities in different types of media are scarce. *Eristalis* eggs are laid in clutches and hatch more or less synchronously within a clutch (Gladis 1994), resulting in a patchy appearance of larvae and making it difficult to obtain useful density measurements. In the study by Mahmoud (1997), mean monthly *Eristalis* larval densities varied from about 3 to about 60 (with a mean of about 24) larvae per 900 cm² surface area in a gravel-bed hydroponic system in Abu-Attwa (Egypt), where the water was 30 cm deep, (approximately 30 to 650, mean 275, larvae per m² of water surface). In a much more extensive study by Ibrahim (1976), *Eristalis* larval densities were investigated in eight different habitat types at 22 study sites throughout Egypt. The highest mean and maximum larval densities of approximately 300 and 940 larvae per m² of water surface, respectively, were found in drain water bodies (Fig. 12).

Study of Campan and Campan (1979) showed that the approach to the oviposition site in *E. tenax* involves a complex interplay of olfactory and visual cues, with different behaviours and reactivities at various stages of ovarian development. The hoverflies response to the smell of manure varied with the

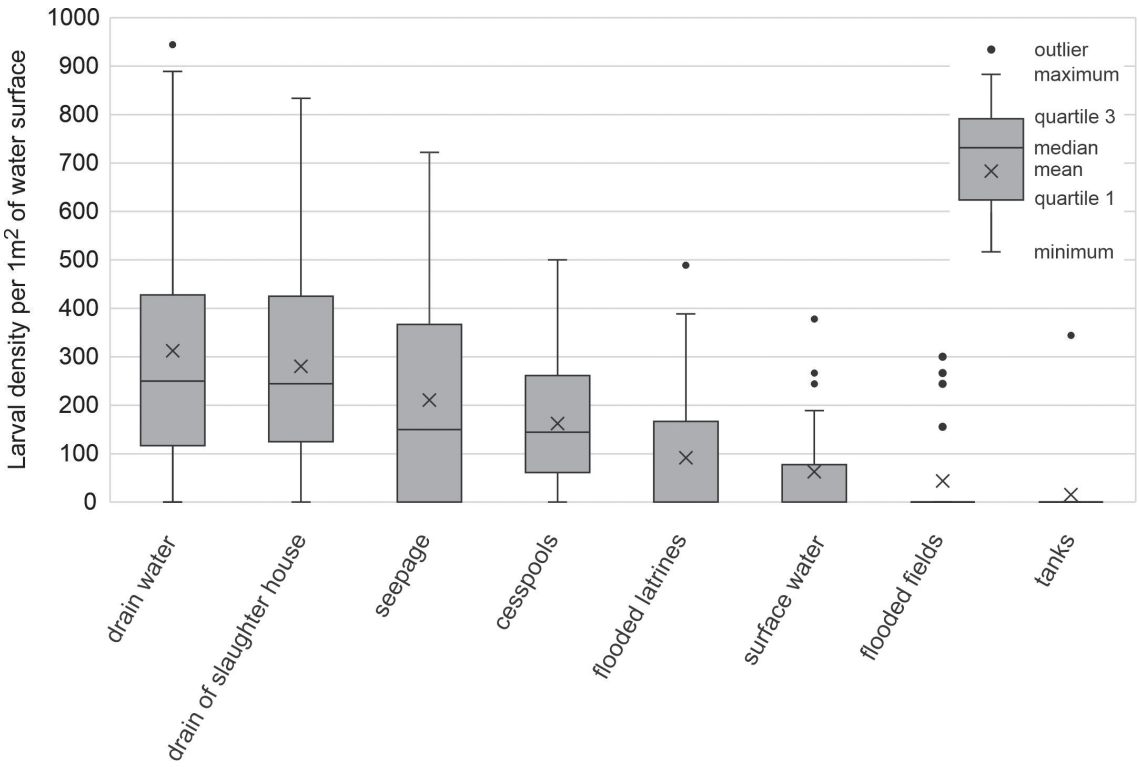

Figure 12. *Eristalis* larval densities in different microhabitats across 22 study sites in Egypt (based on Ibrahim 1976).

stage of oocyte development. Immature females were repelled by the smell, developing females were indifferent, and mature females were attracted to it. The field observations of Campan and Campan (1979) showed that egg-laying in *E. tenax* is not typically performed during a single flight. The study suggests that the approach to the oviposition site involves multiple visits over several days. During these visits, the flies perform various activities such as flying over the manure, exploring the site, and adopting preparatory postures before finally laying eggs. This sequence of behaviours reflects a gradual approach to the egg-laying site, rather than a single, direct flight. In addition, Campan and Campan (1979) observed that not all females that explored the oviposition site ended up laying eggs. Many females performed exploratory behaviors, but then flew away without laying eggs. In addition only a small percentage of marked females returned to the manure site, and those that did often performed the same type of visit multiple times before laying eggs.

Planned implementation in the model

Following Honěk (1993), we assume that the *E. tenax* potential fecundity (potential total number of eggs to be laid) depends linearly on the female"s mass and thus is set at the female"s emergence. As data on individual mass and fecundity were not available for *E. tenax*, we based the linear relationship on the minimum and maximum values reported in the literature (Tables 1, 9), assuming that the minimum reported mass corresponds to the minimum reported fecundity, and the maximum reported mass corresponds to the maximum reported fecundity (Equation 15). Female mass data were taken from the field measurements of Nicholas et al. (2018) (Table 1). As field data on fecundity

was not available for *E. tenax*, we decided to use fecundity data measured in the laboratory from Hurtado (2013), as the percentage of ovipositing females in this study was much higher than in Campoy et al. (2020) (Table 9).

$$N_{Tegg} = 8.782 * M_f - 867.244 \quad \text{Equation 15}$$

where N_{Tegg} is the potential fecundity of a female, and M_f is the mass of a female.

After hibernation (autumn generation) or emergence (spring/summer generation), a female enters a pre-oviposition period. We will divide the pre-oviposition period into two distinct phases: (1) the time required for ovary development and (2) the time required for egg maturation (at the beginning of which mating occurs). The duration of these phases will be tracked separately. This tracking can be achieved by monitoring when a female hoverfly accumulates a specific amount of nutrients (i.e., floral resources) in its gut (i.e., achieves the "reproduction goals"). This artificial construct ensures a consistent tracking mechanism for the gut content associated with each clutch produced by a female.

We assume that the "egg maturation" phase must be repeated for each clutch, while ovary development occurs only once during a female"s lifetime. Following the findings of Gladis (1993, 1994b), we hypothesise that, as in *H. pendulus*, mating in *E. tenax* may occur multiple times, on the day following previous oviposition event. Consequently, mating events are considered an integral part of the "egg maturation" phase. Thus "egg maturation" phase will start with the mating event and end with the oviposition event. Both processes depend on nutrient accumulation, with ovary development requiring a one-time nutrient threshold and egg maturation requiring a nutrient threshold for each clutch. We assume that the same foraging-based resource counter (linked to the rate of gut filling) can be applied to each clutch implying that the target clutch size remains unchanged over time and does not vary with the age of the female. This is a simplifying assumption, as empirical evidence from Campoy et al. (2019) indicates that fecundity in *E. tenax* may vary with age. For the purposes of our model, we further assume that each oviposition event results in the deposition of a single clutch of eggs. According to Gladis (1993, 1994b), oviposition in *H. pendulus* typically concludes with the laying of two to three (or more) clutches of eggs, all deposited on the same day and in close proximity. To simplify our modeling framework, these multiple clutches are treated as a single oviposition unit, and thus considered as one clutch.

Following Honěk (1993), we assume that the nutrient threshold P_{odev} for the "ovary development" phase depends linearly on the female"s mass, as the bigger the female, the more ovaries it has, and the more nutrients she needs to accumulate for the ovary development. We further assume that each female, depending on her mass, has a certain minimum and maximum target number of eggs per clutch to oviposit, which correspond with the minimum and maximum nutrient thresholds, P_{eggmin} and P_{eggmax}, needed for the maturation of eggs. Nutrient thresholds P_{odev}, P_{eggmin} and P_{eggmax} will be expressed as percentages of female"s gut filled with pollen, and set during the calibration process.

The actual clutch size will vary from the targeted maximum due to environmental factors such as spatial and temporal distribution of floral resources and weather conditions that influence daily foraging activities, and thus the daily intake of nutrients needed for the maturation of eggs (see "Foraging"

section for details). These factors, along with the potential fecundity of the female, will determine the number of clutches produced. Under permitting weather conditions, the hoverfly female will gather a certain amount of pollen per day (from various resource patches reached in multiple movement bouts) depending on the availability of food resources around its location. She will continue feeding on pollen until the minimum nutrient threshold P_{eggmin} is achieved and the probability of continuing foraging p_f is above zero or until the maximum nutrient threshold P_{eggmax} is achieved. The probability of continuing foraging p_f or, in other words, the willingness to continue foraging will be set to 1 until the optimal duration of maturation of eggs period (D_{Mopt}) is reached and will drop afterwards to reach zero when the maximum duration of maturation of eggs period (D_{Mmax}) is reached (Fig. 13). The optimal and maximum duration of maturation of eggs period, D_{Mopt} and D_{Mmax}, will be initially set based of reproductive parameters of *E. tenax* measured in the laboratory conditions (Table 9). The shape of the probability curve will be calibrated to derive distributions of egg-laying patterns. The calibration of nutrient thresholds and probability p_f distribution will need to consider the duration of the pre-oviposition period, intervals between clutches, and egg clutch size, representing the field/laboratory situation (Table 9). Here, we assume that the period needed to develop the ovaries can be calculated by identifying the patterns of the duration of pre-oviposition periods and the interval between clutches.

Once the maturation of eggs is finished (according to the rules described above), the female will move to the egg-laying habitat, and the oviposition will be triggered. As this is an energetically demanding activity, it is only triggered if enough nectar is collected in the gut (nutrient threshold N_{ovi} is reached; to be calibrated). If not, the female will continue feeding on nectar till the required amount is reached. The size of a clutch will depend on the percentage of the gut filled with the pollen, assuming the linear relationship. We assume that if the size of a clutch is smaller than the maximum clutch size, the remaining egg load is "lost" (i.e. we assume the phenomenon of egg resorption in *E. tenax*). This means that the total number of eggs laid by a female in all clutches may differ from her potential fecundity. Once the clutch has been laid, foraging activity is resumed and the reproductive behaviour is repeated until no eggs remain to be laid.

For oviposition, a map of larval habitats is needed, as eggs are laid close to these habitats. We will assume that each patch in a landscape is characterized by a maximum density of *E. tenax* larvae L_{dmax}, which corresponds to a maximum egg density E_{dmax}, above which a clutch oviposition is no longer possible. Unfortunately, studies on the effect of habitat type and quality on *Eristalis* larval densities are very scarce and practically limited to laboratory studies analyzing the survival and development time of larvae cultured in different growing media. In addition, it is very difficult to properly map possible larval habitats in a landscape because *Eristalis* larvae are quite versatile and can adapt to different environments as long as there is sufficient organic matter for them to feed on. They can be found in drainage ditches, lagoons and manure pits on farms, stagnant water of various origins, compost heaps or rooting vegetation. Therefore, instead of directly mapping *Eristalis* larval habitats, we propose to characterize each landscape element by a larval habitat quality index L_q, based on a general classification of landscape elements according to their suitability as habitats

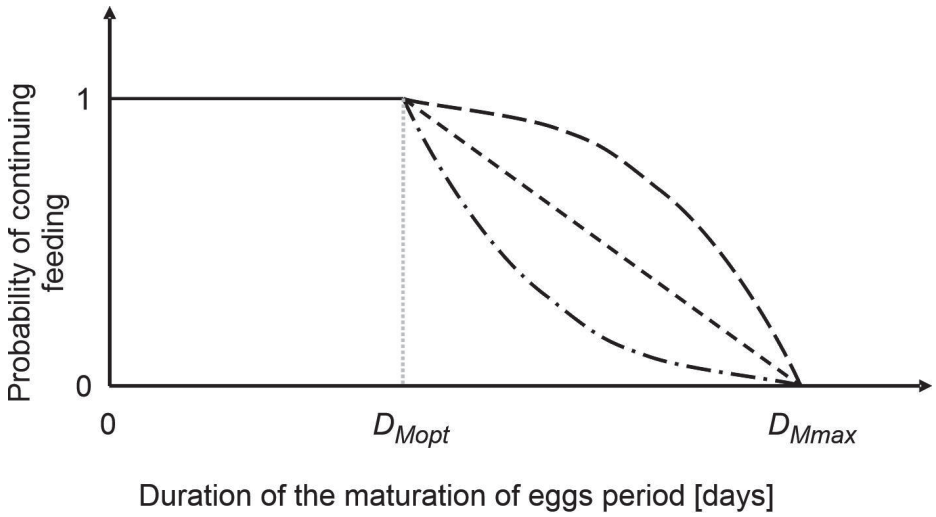

Figure 13. Probability of *Eristalis tenax* continuing pollen feeding during the maturation of eggs period. D_{Mopt}, D_{Mmax} – optimum and maximum duration of the maturation of eggs period, respectively. Maturation of eggs period here is understood as a time needed to gather enough pollen resources for the maturation of eggs forming one clutch. Together with the time needed to develop the ovaries, it forms the pre-oviposition period (see the "Reproduction" section for details).

for *Eristalis* larvae (Table 6), but also taking into account the moisture conditions resulting from the properties of the soils and the local topography, as well as the current meteorological conditions (i.e. the deviation of the precipitation regime from normal conditions). Thus, the larval habitat quality index L_q of a habitat patch p will be calculated as a combination of larval habitat score h_s defined based on habitat classification in terms of suitability as a larval habitat, and soil moisture score m_s (averaged across the patch area), modified by the precipitation regime score p_s at day d (Equation 16).

$$L_{q,p} = h_s \times \frac{\sum_{i=1}^{n} m_s}{n} \times p_{s,d} \qquad \text{Equation 16}$$

The soil moisture score m_s (initially ranging from 1 to 5, with 1 representing very low soil moisture and 5 representing very high soil moisture) will be calculated for each pixel of a raster map of the landscape, and then averaged over all n pixels of a given habitat patch to represent the patch-level value. The score will be derived from the soil moisture proxy model by integrating three components, initially with equal weights: slope, total available water of a soil, and solar radiation (as proposed in Brown 2016). Slope is inversely related to soil moisture in the model, as the steeper the slope, the more runoff and the less water infiltration. Solar radiation is an alternative measure of aspect and may serve as a proxy for varying levels of potential evapotranspiration during a growing season (Jensen and Haise 1963; Nikolaou et al. 2023). Solar radiation is also inversely related to soil moisture in the model. Total available water (TAW), or plant-available water, quantifies the amount of water available to plants that the soil can hold (de Melo et al. 2023). The bigger the TAW, the wetter the soil and better plant growth conditions. TAW values for different soil particle-size classes (according to FAO 2006) used in ALMaSS will be defined based on the soil textural triangle of TAW predicted by the FAO method by de Melo et al. (2023) (Table 7).

Table 6. Habitat classification in terms of suitability as a larval habitat. Larval habitat types (A, B, and C) will have assigned larval habitat scores (initially from 1 to 3). Each column provides the list of ALMaSS habitat types assigned initially to each larval habitat type. The habitat types are defined as Types of Landscape Elements (Topping and Duan 2024a) using the names provided here preceded by tole_. The tole_ types not mentioned in this table are assumed to be in the category of zero as not suitable as larval habitat.

Low (A)	Medium (B)	High (C)
Garden	YoungForest	DeciduousForest
Parkland	MixedForest	Pond
UrbanPark	NaturalGrassWet	DrainageDitch
ConiferousForest	DrainageDitch	Stream
RiversidePlants	ForestAisle	Fields in animals and vegetable farms
Wasteland	WoodlandMargin	Marsh
	PermPastureTussockyWet	
	FarmYoungForest	
	OFarmYoungForest	
	PitDisused	
	Fields in all other farm types	

Table 7. Total available water (TAW) for different soil particle-size classes (according to FAO 2006) used in ALMaSS. TAW ranges were obtained from soil textural triangle of TAW predicted by the FAO method by de Melo et al. (2023).

AlmCode SoilType	FAO texture code	Description	Available water-holding capacity (AWC) [m^3/m^3]
1	S	Sand (unspecified)	0.02-0.08
2	LS	Loamy sand	0.06-0.14
3	SL	Sandy loam	0.14-0.24
10	SC	Sandy clay	0.14-0.18
4	SCL	Sandy clay loam	0.16-0.20
12	C	Clay	0.14-0.24
13	HC	Heavy clay	0.14-0.24
7	CL	Clay loam	0.18-0.28
8	L	Loam	0.20-0.28
11	SiC	Silty clay	0.24-0.28
6	SiCL	Silt clay loam	0.24-0.30
5	SiL	Silt loam	0.28-0.36
9	Si	Silt	0.36-0.40

We assume that the habitat patches that are potentially suitable for *E. tenax* larval development (Table 6) may differ in terms of topography and soil properties, which influence the occurrence of microhabitats suitable for larval development within the patches. This can be further modified by the current meteorological conditions, i.e., if the precipitation regime is wetter or drier than normal, expressed by the precipitation regime score p_s in Equation 15. The precipitation regime score p_s will be derived from the Standardized Precipitation Index (SPI) (McKee et al. 1993), which measures precipitation anomalies

(deviations from the mean) at a given location, based on a comparison of observed total precipitation amounts for an accumulation period of interest (e.g. 1, 3, 12, 48 months), with the long-term historical precipitation record for that period. It is a commonly used indicator for the detection and characterization of meteorological droughts. Here, we will use the short-term SPI (i.e., calculated for shorter accumulation periods) because it can be used as an indicator of immediate effects such as reduced soil moisture, and flow in smaller streams and ponds. Relative scores of SPI values will be used to modify the larval habitat quality, taking into account drier or wetter hydrological conditions as normal (Table 8). Raster maps of SPI (spatial resolution of 0.25°, temporal resolution of 10 days) can be obtained from the European Drought Observatory of the Copernicus programme (https://drought.emergency.copernicus.eu/).

The larval habitat quality index L_q (initially from 0 to 30) will be linked to maximum larval density L_{dmax} via a linear relationship, i.e., assuming a linear relationship between minimum and maximum larval densities observed in the field and (see Table 4) and larval habitat quality (Equation 17).

$$L_{dmax,p}(L_{q,p}) = [A_p \times \frac{L_{d(fieldmax)} - L_{d(fieldmin)}}{L_{qmax} - L_{qmin}} \times (L_{q,p} - L_{qmin}) + L_{d(fieldmin)}] \times r \quad \text{Equation 17}$$

where A_p is area of habitat patch p, $L_{d(fieldmin)}$ and $L_{d(fieldmax)}$ are minimum and maximum larval densities per m^2 possible to be reached in larval habitats of different qualities (e.g., with different amount of organic matter), and L_{qmin} and L_{qmax} are minimum and maximum values of larval habitat quality. $L_{d(fieldmin)}$ and $L_{d(fieldmax)}$ will be initially set at 30 and 940 larvae per m^2 (according to studies by Ibrahim 1976 and Mahmoud 1997, which examined the densities of *Eristalis* species larvae in different microhabitats across Egypt; see Table 4), but may be changed in the future calibration process or if new field data become available. A scalar r will be used ($0 < r < 1$) to scale down the larval density values, as the densities measured in the field were not obtained using a random sampling method (i.e. sampling was targeted to those microhabitats or parts thereof where larvae were observed), and thus their direct conversion to densities per unit area of an entire habitat patch would result in a (rather significant) overestimation. Scalar r will be set during the calibration process.

Table 8. The classification scheme for the Standardized Precipitation Index (SPI) (according to the European Drought Observatory; https://drought.emergency.copernicus.eu/data/factsheets/factsheet_spi.pdf) with proposed relative scores ps applied to modify the larval habitat quality.

Range of SPI values	Precipitation regime	Relative score (p_s)
≤ -2	Extremely dry	0.5
-2 – -1.5	Very dry	0.7
-1.5 – -1	Moderately dry	0.9
-1 – 1	Normal precipitation	1
1 – 1.5	Moderately wet	1.1
1.5 – 2	Very wet	1.5
≥ 2	Extremely wet	2

Table 9. Reproductive parameters of *Eristalis tenax* across different studies.

% of ovipositing females	Pre-oviposition period (days)	Oviposition period (days)	Female longevity (days)	Mean number of eggs/ female	Mean number of clutches/ female	Mean number of eggs/ clutch	Mean number of eggs/ first clutch	Interval between clutches (days)	Reference
						200.85 (196.4–207.1)			Upchurch et al. (2023)
66.6	21 (15-29)	6.6 (1-26)	46 (18-72)	366 (90-775)	2 (1-5)		201 (60-265)	6.4 (2-12)	Hurtado (2013)
31	26 (19-38)			191 (61-1737)	4 (2-8)				Campoy et al. (2020)
	10		60	3000					Dolley et al. (1933)
	14		up to 120						Gladis (1994)
51							100-200		Heal (1979)

Dispersal

Daily distances of adults

Drone flies begin their adult stage with obligatory dispersal, during which they leave their place of emergence and virtually never return (Wellington and Fitzpatrick 1981). Males are territorial, but only in the summer generation and not in the autumn generation. This territoriality means "an increasing attachment to one particular site, e.g. a few leaves and flowers of one plant". Territorial area is from one site of 0.36 m^2 to several sites scattered over 500 m^2 (Wellington and Fitzpatrick 1981).

Only limited information on distances travelled daily by hoverflies is available. In the capture-recapture studies, non-migrant syrphids travelled distances of up to 400 m (most flies dispersed up to 100 m after release) (Conn 1976; Wratten et al. 2003) with a speed of 12–18 km/h (Aubert et al. 1969). In a field study of Wratten et al. (2003), distances travelled by *Melanostoma fasciatum* (Macquart, 1850) (New Zealand hoverfly species of 6–7 mm length), *Episyrphus balteatus* (De Geer, 1776), and *M. corollae* (United Kingdom hoverfly species of 6–10.25 mm and 7–10.5 mm length, respectively) from a *Phacelia* strip were investigated (Fig. 14). This study was based on analysing the gut contents of hoverflies caught in traps placed at different distances from the food source. Thus, what was actually measured was the displacement from the food source, from which it is difficult to infer the actual distance travelled by the hoverflies per day, especially as the traps were only emptied every seven days.

Collett and Land (1978) measured the *E. tenax* fight behaviour and velocities in the field as being at least 10 m/s but for short periods of time only. However, only flies that are already airborne can reach these speeds; they are likely to fly much slower between flowers during foraging. Golding and Edmunds (2000) measured the time droneflies (*E. tenax*, *E. pertinax*, *E. arbustoeum and E. nemorum*) spend on individual flowers and the time spent on flying between flowers, finding that it was more similar to that of honeybees than to the times of other hymenopterans and dipterans. The time spent on individual flowers depended on the flower type and varied between 5 to 16 seconds. The time spent flying between flowers also depended on flower type and varied between 1.3 to 3.7 seconds (but mostly around 1.5 seconds).

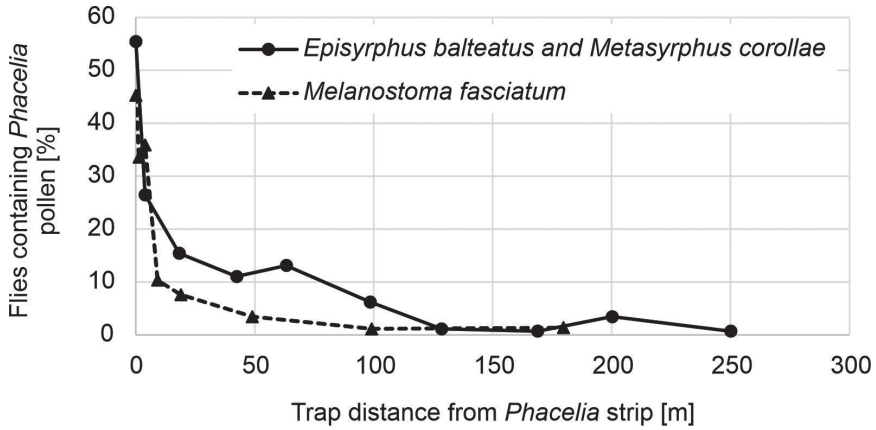

Figure 14. Displacement from a *Phacelia* strip of hoverflies *Melanostoma fasciatum* (New Zealand species) and *Episyrphus balteatus* and *Metasyrphus corollae* (United Kingdom species) (based on Wratten et al. 2003). Results from a field experiments in which hoverflies were caught in traps located at certain distances from the *Phacelia* strip. The traps were emptied every 7 days.

Francuski et al. (2014) studied the landscape genetics of *E. tenax* in a spatially heterogeneous landscape of Durmitor Mountain (Montenegro). Their sampling points covered a broad range of altitudes and vegetation structures, from deciduous and coniferous forests to alpine meadows). They found a lack of population structure in the studied area, suggesting that *E. tenax* dispersal ability is sufficient to establish gene flow over a network of habitats involving the whole study area. The observed lack of isolation by geographical distance suggests that dispersal ability is not the key factor determining distributions of *E. tenax* at the spatial scale studied (15 × 15 km). Similar studies on *E. tenax* populations conducted on even larger spatial scales, encompassing populations from the Central-Eastern Mediterranean (Francuski et al. 2013a) and along a north-south European gradient from Finland through Switzerland to Serbia (Francuski et al. 2013b), also demonstrated the absence of large-scale geographic structuring. Therefore, it seems that the species is restricted in its distribution by the availability of suitable habitat rather than the ability of a species to disperse between available habitat patches.

Long-distance migrations of the autumn generation

Adults are capable of extensive, long-distance migration (Bailes et al. 2018) and can fly continuously over distances for at least 75 km across the open ocean (Krčmar et al. 2010). In Europe, they can migrate north to avoid hot summers before returning south in autumn (Francuski et al. 2014; Francuski and Milankov 2015). A comprehensive review by Reynolds et al. (2024) consolidates robust evidence for long-distance migration of *E. tenax* in Europe, North America, and Oceania. Despite the classification of *E. tenax* as a weakly migratory species by Hlaváček et al. (2022), long-term observational studies, such as the 12-year investigation by Aubert et al. (1976) and the extensive 50-year monitoring programme in Germany led by Gatter (Gatter 1976; Gatter et al. 1990, 2020), underscore the ecological relevance of migratory behaviour in this species. Further supporting this migratory capacity, Hawkes et al. (2022) demonstrated the potential for long-distance pollen transport by *E. tenax*, indicating functional connectivity between distant habitats.

Tomlison and Menz (2015) explored partial migration in hoverflies, linking migratory propensity to physiological traits such as metabolic rate, thermal tolerance, and rates of water loss. Their findings suggest that most individuals possess the physiological capacity for migration, with inter-individual variation, particularly among females, potentially reflecting differential adaptation to thermal environments and reproductive strategies. However, the relative proportion of migratory versus resident individuals within populations remains unknown. Reynolds et al. (2024) propose that this ratio is likely modulated by complex interactions between seasonal temperature regimes and photoperiodic cues.

Planned implementation in the model

We will treat *E. tenax* as a partially migratory species. Specifically, we assume that the proportion of females from the autumn generation will exhibit migratory behaviour, departing from the local landscape after mating. A given female from the autumn generation will initiate migration movement with a defined probability p_{mig}.

We will distinguish between local movements within the flower patch (considered under "feeding time") and movements between floral patches (considered under "flight time"; see "Diurnal activity" for more details). The former type of movement will not be tracked in the model. The maximum daily dispersal ability D_{tmax} (for movements between floral patches) will be calculated from the available daily flight time (h_m) and the flight speed v achieved by *E. tenax* hoverflies already in the air (Equation 18). Dispersal activity will be tracked individually for each hoverfly, both in terms of time spent and distance travelled, and once daily limits are reached a hoverfly will suspend its activity for that day.

$$D_{tmax} = h_m \times v \qquad \text{Equation 18}$$

We assume mean v being set to 10 m/s, as measured by Collett and Land (1978). In addition, an individual variation will be included around this mean speed (+/- 10%).

Four types of dispersal actions will be considered:

1. Random movement/displacement after the emergence.
2. Local daily foraging movements (summed up to a maximum daily dispersal ability) carried out in N_f bouts. This movement is driven by the availability and distance to foraging resources.
3. Movement to a larval habitat once the female is ready for oviposition (i.e., foraging goals have been achieved). This movement is driven by the availability, attractiveness and distance to larval habitats, subject to local daily foraging movements providing sufficient resources.
4. Movement to a hibernation site, subject to local daily foraging movements providing sufficient resource.

We plan to represent the movement using the following rules:

1. Determine the reproduction state of the female, i.e., mating, development of ovaries, egg maturation or oviposition. The reproduction state is updated daily depending on the foraging status and can be switched

if certain reproduction goals are achieved (see “Reproduction” section for details).
2. If reproduction goals are not achieved, then foraging activity is triggered. Depending on the state, the foraging goal is set, i.e., during mating and oviposition, the foraging goal is a 20:80 pollen-to-nectar ratio, whilst, during the development of ovaries and egg maturation, it is a 90:10 pollen-to-nectar ratio. Foraging movement is continued till the reproduction goals are achieved.
3. If reproduction goals are achieved, then the availability and attractiveness of larval habitat (possibility of oviposit) should be evaluated.
4. If the attractiveness of larval habitats is enough for oviposition, lay a clutch; otherwise, move to the larval habitat. Searching for larval habitat will continue until the attractiveness of larval habitat is enough for oviposition.
5. Once a clutch is laid, the current reproductive potential is assessed, and if any eggs are left to lay, then continue the behaviours on the following day; otherwise, die.

The flow diagram for this behaviour is described in Fig. 15. This behaviour requires the specification of four functions: one for setting the forage goal, the second for determining the forage status (in relation to reproduction goals), the third for accepting a habitat patch for foraging, and the fourth for larval habitat acceptance. The function for setting the forage goal is expressed in terms of the ratio of pollen to nectar. Two foraging goals are possible, either 90:10 or 20:80 pollen to nectar ratio, depending on the behavioural state of the female (see "Foraging" for details). The function for determining the forage status tracks the percentage of gut filling in terms of pollen and nectar (see "Foraging" for details).

The function for determining accepting a given patch for foraging at a given food attractiveness is given by a probability function between two thresholds such that a hoverfly will not accept a given patch for foraging below F_l, a minimum food attractiveness threshold (e.g. 0), and the probability of accepting a patch for foraging then increases linearly to an upper threshold F_h. The values for the probabilities at F_l and F_h would be given as F_{lp} and F_{hp}. The food attractiveness value to drive this function will come from Equation 15. Given the frequent movement of hoverflies between patches, we assume that the probability of leaving a given habitat patch (p_{move}) increases over time with the base probability inversely related to the food attractiveness of the patch (Equation 19). Consequently, patches with higher food attractiveness will have longer occupancy times compared to those with lower food attractiveness, compelling hoverflies to move more frequently when patches are less resource-rich.

$$p_{move}(t,\ F_h) = p_o + k \times t \times F_h^{-1} \qquad \text{Equation 19}$$

where p_0 is the base probability of leaving the habitat, k is a constant that determines how the probability increases with htime, t is the time spent in the habitat patch, and F_h is the food attractiveness of the patch.

The function for determining clutch laying at a given habitat patch is given by a probability function between two thresholds that clutch is not laid below L_l, a minimum larval habitat attractiveness L_a (e.g. 0), and the probability of laying a clutch then increases linearly to an upper threshold L_h. The values for the probabilities at L_l and L_h would be given as L_{lp} and L_{hp} and will be calibrated.

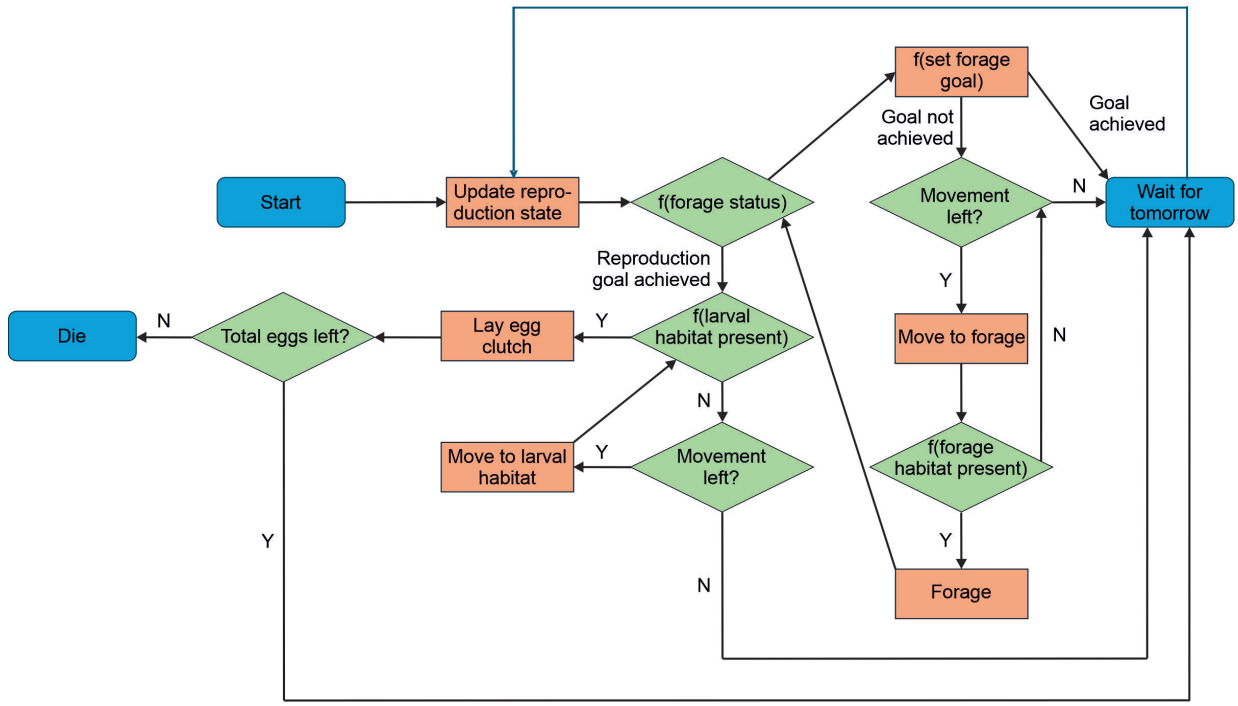

Figure 15. Overview of behavioural decisions related to foraging and egg clutch-laying movement of *Eristalis tenax*. Each move also uses up the distance allocation for the day, which when used will result in stopping movement for the day (hibernation and migration behaviour not included, see text).

The larval habitat attractiveness value L_a to drive this function will come from larval habitat quality (Equation 16) modified by factor c ($0 < c < 1$) indicating the presence of other clutches in the same habitat patch p (Equation 20).

$$L_{a,p} = L_{q,p} \times c_p \qquad \text{Equation 20}$$

Factor c allows to account for density-dependent oviposition, as clutch-size optimality models (e.g., Iwasa 1984; Wilson and Lessells 1994) suggest that insects may avoid laying clutches in areas with high egg densities to reduce competition for food and space for their offspring and to reduce the risk of predation. We are unaware of any studies that confirm that such strategy exists in saprophagous flies, so this factor will be set to 1 in the initial version of the model. Other settings may be used to test the effect of density-dependent oviposition on the results of the model, or if new evidence becomes available for saprophagous hoverflies.

Fig. 13 does not include hibernation and migration behaviours. These behaviours are triggered by the assessment of the reproduction state. After mating, if this is the autumn generation, the female initiates hibernation or migration movement. In case of hibernation, the behaviour follows the same procedure as Fig. 15 but replacing "larval habitat" with "hibernation habitat" and "lay egg clutch" with "enter the hibernation state". Once in hibernation, the female switches the state to the development of ovaries only after the emergence from hibernation. If it is the spring/summer generation, the female goes directly from mating to the development of ovaries. In the case of migration, a female is assumed to leave the landscape and is consequently removed from the modelled population. There is a certain probability p_{mig} of a certain female migrating instead of overwintering.

Overwintering/hibernation

Part of the autumn (second) generation of *E. tenax* not migrating, overwinters. These individuals are predominantly adult females that have been inseminated and subsequently enter a facultative reproductive diapause. This diapause phase is characterized by a cessation of ovarian development and a marked hypertrophy of the fat body (Hondelmann and Poehling 2007; Tomlinson and Menz 2015; Campoy et al. 2022). Overwintering males are rare, as most die in the autumn (Kendall and Stradling 1972). Hibernation lasts from late autumn to early spring. In nature, fertilised females hibernate in groups (up to 20 individuals) in dark and humid places such as caves or crevices in rocks and buildings. These provide shelter from adverse climatic conditions in winter, i.e. stable humidity and temperature conditions that are less affected by the wide variations in air temperature outside. Laboratory experiments by Bressin (1999) showed that overwintering *E. tenax* hoverflies are water-stressed, so selecting overwintering sites with high humidity allows them to limit water losses, as does overwintering in clusters. Thus, certain high levels of humidity (Kendall and Stradling 1972) and darkness are required for a site to be suitable for overwintering. The relative humidity of hibernacula observed by Bressin (1999) was over 90%.

It appears that both the onset and termination of overwintering are primarily controlled by temperature, although day length may also play a role, with decreasing photoperiod inducing overwintering and increasing photoperiod signalling the time to leave the site (Siuda 1963, after Bressin 1999; Moog and Ernst 1978; Davenport 1992). However, daylight is not itself the trigger; it acts as a secondary stimulus to prevent flies from leaving hibernacula too early if the temperature is high enough (Bressin 1999).

In Scotland, Bressin (1999) observed that the onset and end of hibernation were not short periods but extended over several weeks (Figs 16, 17). While some individuals began hibernation in mid-September, others were still active, feeding and foraging until mid-November. The increase in the number of hoverflies settling in the overwintering site corresponded to a decrease in temperature. Under laboratory conditions, hoverflies enter hibernation at 8–10 °C (Bressin 1999). In Scotland, the number of overwintering *E. tenax* began to decline sharply from mid-February, corresponding to a significant rise in temperature. Bressin (1999) suggested that a sustained high temperature (i.e. for at least a few days) is required. This suggestion is supported by the slow response of crevice temperatures to outside temperatures. Different "trigger" ambient temperatures for the end of hibernation have been reported in the literature. Bressin (1999) reported 13 °C in Scotland, while Siuda (1963) reported a much lower temperature of 5 °C in Poland.

Planned implementation in the model

The landscape features that hoverflies are looking for in the search for hibernation places are types of landscape elements connected with rocks and caves, forest edges (tree bark and crevices), hedgerows and shrubs with dense vegetation providing good hiding spots, and single-housing settlement areas with gardens, particularly those with dense vegetation.

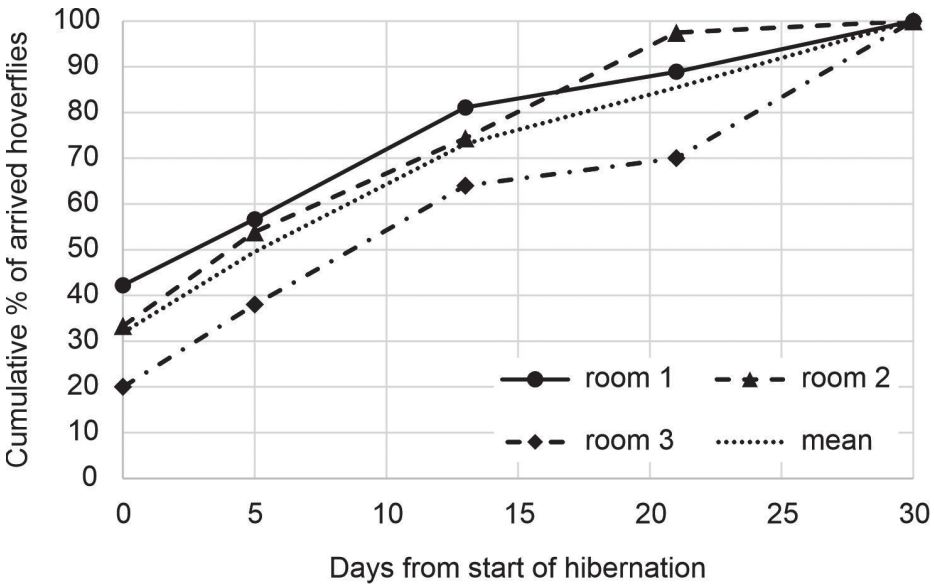

Figure 16. Cumulative percentage of *Eristalis tenax* individuals arriving at the hibernation site as a function of the number of days since the beginning of hibernation period. Based on field observations of Bressin (1999) of hoverflies hibernating in different rooms of ruins of Newark Castle (Scotland) in winter 1997/1998.

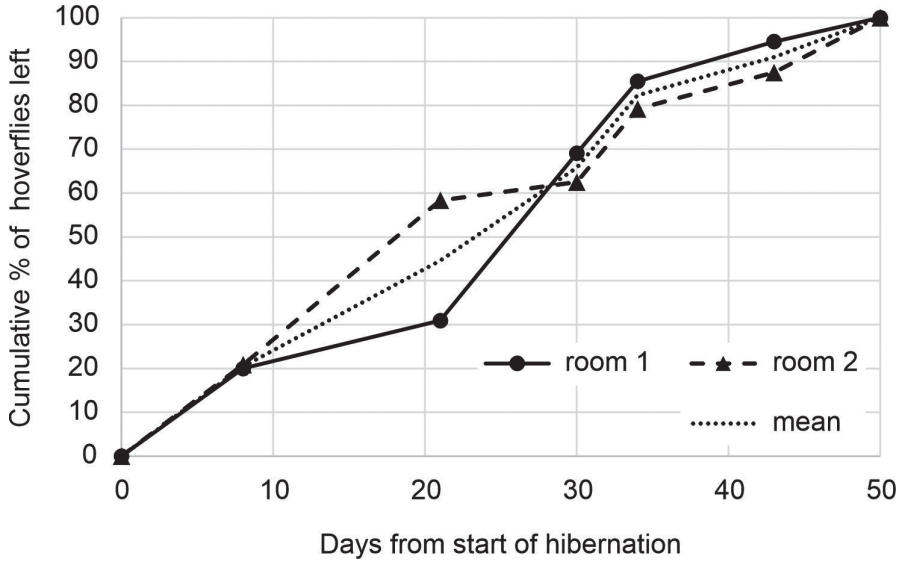

Figure 17. Cumulative percentage of *Eristalis tenax* individuals leaving the hibernation site as a function of the number of days since the end of hibernation period. Based on field observations of Bressin (1999) of hoverflies hibernating in different rooms of ruins of Newark Castle (Scotland) in winter 1997/1998.

A certain number of days (H_{days}) with minimum night temperatures below a threshold (Th_{start}) will be required to initiate hibernation of *E. tenax*. The distribution of the number of individuals entering the hibernation state will be implemented according to field data from Bressin (1999) (Fig. 16). In addition, to account for the effect of photoperiod, a threshold date H_{date} after which the hibernation is mandatory will be applied. Based on field observations of Bressin (1999), H_{days}, Th_{start} will be initially set to 5 days and 10 °C, respectively, and H_{date} will be set to 1st of November.

Emergence from hibernation will also be related to temperature. A certain number of days (E_{days}) with maximum day temperatures above a threshold (Th_{end}) will be required; however, emergence will also be restricted by date, not being earlier than a given day (E_{date}). The distribution of the number of individuals leaving the hibernation state will be implemented according to field data from Bressin (1999) (Fig. 17). Based on field observations of Bressin (1999), E_{days} and Th_{end} will be initially set to 5 days and 10 °C, respectively, and E_{date} will be set to 10th of February.

Body size dependence

It has been shown that developmental environments with low nutrient quality or quantity (i.e. nutritional stress) cause increased duration of preimaginal stages, decreased survival, and reduced adult size and fecundity in many dipteran species (Stearns 1992; Gleiser et al. 2000). For example, nutritional stress in *Drosophila melanogaster* caused a 20% reduction in viability, a 70% increase in total egg-to-adult development time, and a 50% reduction in adult weight (Kolss et al. 2009). Hurtado (2013) demonstrated that both larval developmental medium (with constant larval density) and larval density can impact the duration and survival of larval stage, as well as mass of adults in *E. tenax*, confirming that nutritional stress can occur in this species and impact larva"s survival and mass of adults. When tested with pig slurry as a rearing medium, mass of female *E. tenax* adults decreased significantly with increasing larval density (Fig. 18; Equation 21).

$$M_f(L_d) = -0.175 \times L_d + 29.833 \quad \text{Equation 21}$$

where M_f is mass of a female and L_d is larval density.

Planned implementation in the model

From Ludoski et al. (2023), we know that the pupa mass is linearly related to the adult female mass. Thus, if we know that the nutritional stress impacts larval and pupal mass, then we can assume that it directly affects adults mass without calculating the intermediate masses. This is possible since pupal mass is not used directly in the model.

In the model, mass variability will be introduced at the larval stage in the sense that different larval habitats will be assigned different qualities (see section "Reproduction and oviposition"). The quality of larval habitats will be expressed as possible maximum larval densities, and if those are reached, further eggs will not be laid in these habitats. The impact of larval density L_d on the mass of adult female M_f will be determined according to Hurtado (2013) (Fig. 18; Equation 21). This relationship will be scaled to the maximum larval density associated with the habitat (Equation 22):

$$M_f(L_d) = (a + b \times L_d) \times \frac{L_{dmax,h} \times M_{fmax}}{L_{dmaxtotal}} \quad \text{Equation 22}$$

where *a*, and *b* are from a linear regression fitted to Fig. 18 (Equation 21), $L_{dmax,h}$ is the maximum larval density per habitat *h*, $L_{dmaxtotal}$ is the maximum larval density for all habitats, *and* M_{fmax} is the maximum adult female mass.

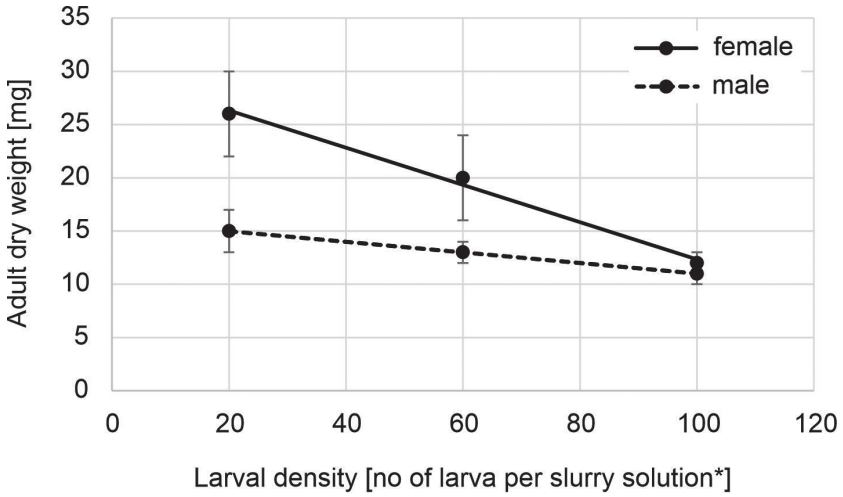

Figure 18. Dependence of *Eristalis tenax* adult dry weight on larval density measured as number of larvae per slurry solution. Fitting linear equation to the data provides model for female mass and larval density (Equation 21; R^2 = 0.99). The difference between dry weight of adult male at different larval densities was not significant. Based on Hurtado (2013). * Slurry solution: 75 g of pig slurry mixed with 200 ml of water in 10.5 × 10.5 × 5 cm container of 0.5 l volume.

Mortality

Mortality of the egg-to-pupa stages

Information on egg survival for *E. tenax* is scarce, but the egg cluster viability is rather high, estimated to be about 86–100% by Bressin (1999). There is also limited information on larval survival, but it seems that this is impacted mostly by the temperature (Heal 1989; Ottenheim et al. 1996), and to a lesser degree by larval density and food/environment type (Hurtado 2013). The data summarising the dependence of larval survival on the temperature are presented in Table 10 and Fig. 19.

There was sufficient data to estimate the thermal performance curve for pupal survival, based on three publications: Heal (1989), Hurtado (2013) and Daňková et al. (2023) (Table 10). Thermal performance curves for pupal survival were estimated using 24 models with rTPC R package (Padfield et al. 2024) as described in Padfield et al. (2021). Table 11 shows the estimation for those models for which it was possible. The graphical representation of four best-performing models is shown in Fig. 20.

Planned implementation in the model

Background mortality will be defined separately for the egg-to-pupa stages. This mortality is a daily probability applied at the start of each daily time step. For the egg stage, due to limited data inputs, the daily background mortality will be drawn from a uniform distribution from a range between 0 and p_{megg}, where p_{megg} (based on Bressin 1999) is calculated as (Equation 23):

$$(p_{megg})^d = 0.14 \qquad \text{Equation 23}$$

where d in the developmental time of the egg stage (in days).

Table 10. Summary of survival of subsequent life stages of *Eristalis tenax*.

Stage	Temperature conditions [°C]	Survival [%]	Species	Reference
Egg	variable	86-100	*E. tenax*	Bressin (1999)
Larva	12	12.1	*E. arbustorum*	Ottenheim et al. (1996)
	20	81.2		
	21	83.3	*E. tenax*	Basley et al. (2018)
	20	90.0	*E. tenax*	Kandem et al. (2024)
	20	80	*E. tenax*	Hurtado (2013)
	20	65.8		
	20	74.4		
	Low (< 10 °C)	32.5	*E. tenax*	Heal (1989)
	High (> 20 °C)	67.5		
Pupa	25	94.6	*E. tenax*	Heal (1989)
	25	87.7		
	25	75.6		
	25	71		
	25	43.5		
	25	92.1		
	25	100		
	25	93.1		
	11	98.3		
	17	82.2		
	15	88.2		
	10	58		
	9	35.6		
	18	81.3		
	14	60.9		
	14	87.5		
	19	90.9		
	10	75		
	14	100		
	16	68.9		
	9	68.6		
	12.5	93.3		
	26	60.7		
	20	92.5	*E. tenax*	Hurtado (2013)
	23	95.1	*E. tenax*	Daňková et al. (2023)
	25	85.7		
	12	56.8		
	17	76.1		
	25	48.6		
	12	71.9		
	17	95		
	25	65.9		
	12	78.7		
	17	79.7		
	25	66.7		
	12	85.5		
	17	87.5		
	25	35.4		
	23	85.6		
	23	86.8		
	10	30		
	10	2.5		

Table 11. Parameters of the thermal performance curves fitted to the pupa mortality for *Eristalis tenax*. CT_{Mpupa_min}, CT_{Mpupa_max} – critical thermal minima and maxima; T_{Mpupa_opt} – thermal optima for mortality. Model abbreviations follow the convention used in rTPC R package (Padfield et al. 2024).

Model	CT_{Mpupa_min}	T_{Mpupa_opt}	CT_{Mpupa_max}
briere2_1999	0	26	40
delong_2017	-2	19.1	42.6
gaussian_1987	-2.8	19.2	41.2
joehnk_2008	4	19.5	31.4
kamykowski_1985	0.9	24.7	29.5
lactin2_1995	6.7	22.8	26
lrf_1991	5.0	19.1	33.1
oneill_1972	-3.2	19.3	40.5
pawar_2018	-27.9	21.1	34
quadratic_2008	5	19.1	33
ratkowsky_1983	2.5	19.2	35.8
thomas_2012	-9.1	21.3	27.1
weibull_1995	6.6	18.3	52.1

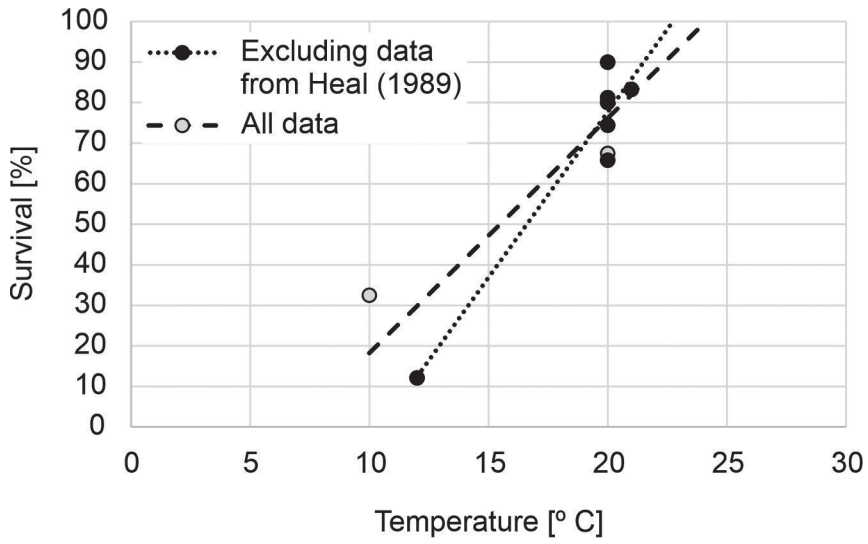

Figure 19. Dependence on *Eristalis* larva survival on temperature, based on Table 10. The black dots are based on the data from Table 10 with the exclusion of values reported by Heal (1989). The grey dots and dashed regression line is based on all the data presented in Table 10. Here we assume that survival reported by Heal (1989) for "low" and "high" temperature conditions depict the situation for 10 and 20 °C, respectively.

For the larva stage, the daily background mortality p_{mlarva} will depend on both the temperature and the larval density (Equation 24).

$$p_{mlarva} = p_{mlarvat} \times p_{mlarvaLd} \quad \text{Equation 24}$$

The temperature-dependent mortality $p_{mlarvat}$ will be calculated based on the linear relationship from Fig. 19, taking into account data from Ottenheim et al. (1996), Hurtado (2013), Basley et al. (2018), and Kandem et al. (2024) (Equation 25).

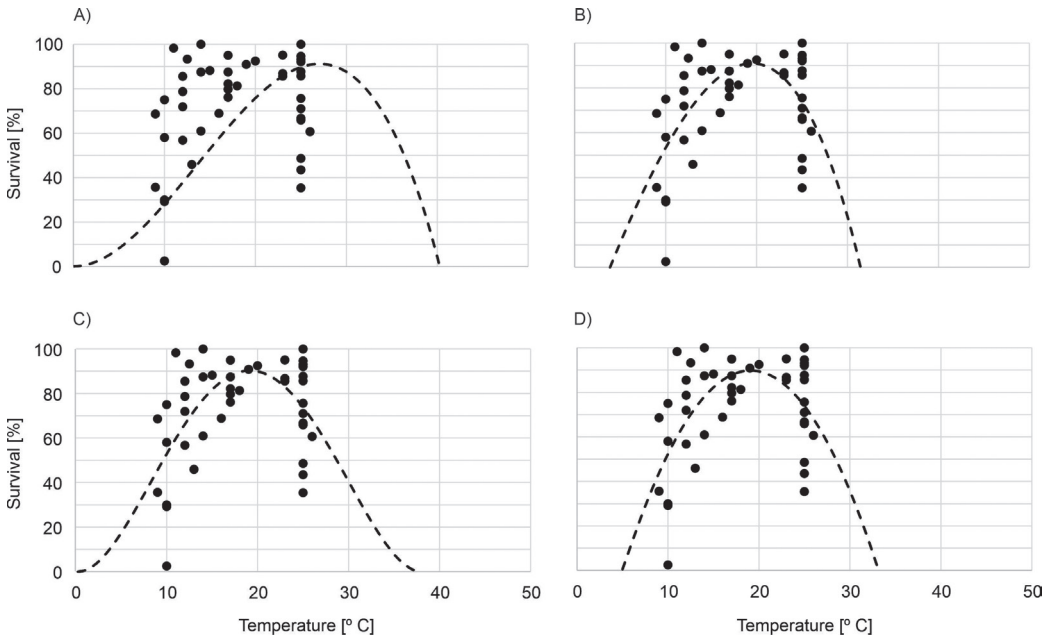

Figure 20. Relationship between temperature and pupa survival of *Eristalis tenax* according to four best-performing models presented in Table 11: A) briere2_1999, (B) lactin2_1995, (C) lrf_1991, and (D) ratkowsky_1983. The input (measured) data are presented as black dots. The input (measured) data are presented as orange dots. Performance of the models expressed as R^2 was 0.11 for briere2_1999, 0.15 for lactin2_1995, 0.30 for ratkowsky_1983, and 0.31 for lrf_1991. Names of the thermal performance curves models after Padfield et al. (2024).

$$S_{larva}(T) = 8.16 \times T - 85.50 \quad \text{Equation 25}$$

where S_{larva} is larva survival, and T is temperature.

The larval density-dependent mortality $p_{mlarvaLd}$ will be calculated based on the linear relationship presented in Equation 3.

The daily background mortality (inverse of survival) in the pupa stage will be related to the temperature using a thermal performance curve model of the Lobry–Rosso–Flandrois (LRF; lrf_1991) (same as the pupal growth). The four parameters in the model represent three cardinal temperatures (the maximum and minimum temperatures T_{Smax} and T_{Smin} at which pupa can survive, and the optimum temperature T_{Sopt}) and the specific rate at the optimum (U_{Sopt}). U_{Sopt} is independent of the three cardinal temperatures, and T is the temperature (Equation 26).

$$S_{\text{pupa}}(T) = u_{\text{Sopt}} \frac{(T - T_{\text{Smax}})(T - T_{\text{Smin}})^2}{(T_{\text{sopt}} - T_{\text{smin}})\left[(T_{\text{sopt}} - T_{\text{Smin}})(T_S - T_{\text{Sopt}}) - (T_{\text{Sopt}} - T_{\text{Smax}})(T_{\text{Sopt}} + T_{\text{Smin}} - 2T)\right]} \quad \text{Equation 26}$$

After fitting the LRF model to our data, the parameters T_{Smin}, T_{Sopt}, T_{Smax} and U_{Sopt} were set to 5.01 °C, 19.08 °C, 33.14 °C and 89.80, respectively.

Pesticide responses

Research on the effects of pesticides in *Eristalis* hoverflies remains limited, with existing studies primarily focusing on neonicotinoids due to their widespread agricultural use and well-documented risks to pollinators. Despite regulatory bans or restrictions on several neonicotinoids within the European Union, these compounds continue to be a central focus of ecotoxicological research, owing to their environmental persistence and ongoing use in certain regions.

In *E. tenax*, imidacloprid has been shown to exert stage- and route-specific toxic effects. Larvae are particularly sensitive to environmentally relevant concentrations, exhibiting dose- and time-dependent mortality, along with biochemical indicators of neurotoxicity and oxidative stress (Kamdem et al. 2024). In contrast, Basley et al. (2018), who investigated the effects of another neonicotinoid, thiamethoxam, reported that chronic exposure reduced larval survival only at high concentrations, with no significant behavioural effects observed in adults. Adult *E. tenax* appear to exhibit relatively high oral tolerance to imidacloprid compared to bees, with sublethal effects on feeding and survival emerging only at elevated doses (Nagloo et al. 2023). These effective doses exceed typical environmental concentrations, suggesting that adverse effects may only arise under extreme or cumulative exposure scenarios. However, when imidacloprid is administered directly to the brain, even sublethal concentrations can impair neural processing in motion-sensitive visual neurons, disrupting direction selectivity and contrast sensitivity, functions essential for flight and navigation (Rigosi & O"Carroll, 2021). Although such exposure routes are not environmentally realistic, these findings underscore the vulnerability of pollinator visual systems to cholinergic pesticides and highlight the need for further investigation into sublethal neurophysiological effects in non-bee pollinators. More recently, Martins et al. (2024) extended this line of research to another syrphid species, *Eristalinus aeneus* (Scopoli, 1763), demonstrating that imidacloprid exposure can also impair survival and behaviour in this ecologically important pollinator.

To date, the effects of insecticides beyond neonicotinoids on *E. tenax* remain largely unstudied, representing a critical gap in our understanding of the species" ecotoxicological sensitivity. This is particularly concerning given the wide array of insecticidal compounds currently used in agricultural landscapes. Findings from studies on neonicotinoid exposure suggest that *E. tenax* may exhibit toxicological responses that differ from those observed in bees, underscoring the importance of including hoverflies in environmental risk assessments.

To simulate pesticide responses in *E. tenax*, we adopt a modelling framework analogous to that used in the development of the ApisRAM honey bee colony model (Duan et al. 2022). Pesticide exposure can occur through the consumption of contaminated nectar, contact, and overspray. By considering these three exposure pathways, we provide an accurate representation of how model hoverflies may encounter pesticides in contaminated environments. $P_B(t)$ is used to represent the accumulated pesticide burden for the individual until day t. $P_B(t)$ is updated by all three exposure paths and is used to calculate the stress caused by pesticide exposure. The new pesticide exposure on day t is represented by $P_N(t)$ which is calculated by Equation 27.

$$P_N(t) = P_I(t) + P_C(t) + P_O(t) \quad \text{Equation 27}$$

where $P_I(t)$ is the new contamination from intake, $P_C(t)$ is from the contact exposure and $P_O(t)$ is from the overspray exposure.

Intake exposure pathway

Foraging hoverflies may be exposed by collecting pollen and nectar from contaminated flowers. The pesticide amount in the consumed resource is represented by $P_I(t)$ and is assumed to move directly to the hoverfly"s body ($P_N(t)$).

Overspray and contact exposure pathways

The overspray exposure pathways are only relevant to any hoverfly stage present at the moment of pesticide spraying. Contact exposure can occur when a mobile stage moves in a contaminated area. In both cases, a simple one-time absorption model is used here, i.e., we assume that the pesticide will be absorbed into the hoverfly"s body once, which is controlled by a parameter for contact and overspray separately.

Contact exposure specifically pertains to foraging adults and occurs when a hoverfly touches a contaminated plant surface during its foraging activities. The amount of pesticide transferred to the body through contact is controlled by two user-defined parameters as shown in Equation 28.

$$P_C = s_c S P_s \quad \text{Equation 28}$$

where P_s is the pesticide amount per square meter on the plant surface, S is a constant representing the area of the hoverfly that is in contact with the surface. Here, we might imagine that foot, abdomen, and wing contact could occur. s_c is the absorption rate that determines the amount of pesticide P_s that will be transferred to the body. This implementation does not consider foraging time, but both parameters can be adjusted to make this approach more or less conservative.

Overspray exclusively occurs when hoverflies (adults or larvae) are active in a field where simultaneous pesticide spraying occurs and/or where drift occurs in the adjacent area. Two parameters, starting time and ending time, for a pesticide spray event are used to control whether overspray can happen. Overspray can only occur if a hoverfly is in the exact location and when the pesticide is being sprayed. When the overspray happens, the contaminated pesticide amount (P_O) going to the hoverfly"s body is calculated using Equation 29.

$$P_O = s_o S a \quad \text{Equation 29}$$

where S represent a proportion of the body surface, as for Equation 28, a is the pesticide spraying application rate, s_o is the absorption rate for overspray.

Toxicology

To determine the effect of the pesticide body burden, the initial model only considers acute mortality. To do this requires three parameters. The first is a threshold for effect, P_t, above which there is a daily probability of mortality P_m. The third threshold D is the daily decay rate of the pesticide in the hoverfly"s body. This approach will implement a first model for implementing pesticide effects and assumes that an ALMaSS or equivalent landscape model is available to generate the pesticide concentration in the nectar and vegetation, as well as overspray.

Other mortalities

There are a number of other mortalities considered in the model, the important one being the daily background mortality of adult hoverflies. Little is known about the background mortality of adult hoverflies under natural conditions.

Parasites on adults appear to be rare, but fungi of the genera *Entomophthora* and *Enipusa* are responsible for some mortality (Gilbert 1986). *E. tenax* can be also parasitised by wasps, *Aspilota ruficornis*, *Rhembobius bifrons*, *and Rhembobius quadrispinus* (Reemer et al. 2009), but little is known about the mortality rates. Hoverflies are also preyed upon by many animals such as birds, toads, wasps, etc., and by carnivorous plants (e.g. the sundew, *Drosera rotundifolia*) (Gilbert 1986). To some extent, adult hoverflies may be protected from predators by their resemblance to wasps or bees, but attacks by wasps are frequently observed (Bressin 1999). Nagloo et al. (2023), who investigated the acute and chronic toxicity of imidacloprid on adult *E. tenax* reared in laboratory conditions, reported that mortality in the control group increased from 0 to 20% with the duration of the experiment. This range of values will be used to adjust the background adult mortality in the model.

With regard to pre-imaginal stages, staphylinid beetles are recognised as natural enemies of syrphid flies and may prey on their egg clutches (Gladis 1994a). In mass-rearing experiments of *E. tenax* conducted by Gladis (1994a), several small staphylinid species, including *Aleochara brevipennis*, *Aleochara lanuginosa*, and *Philonthus politus*, were documented feeding on *E. tenax* larvae. These mortalities are, however, included in the general mortality rates of the egg-to-pupa stages.

The overwintering mortality test is carried out only once, at the end of the overwintering period (before emergence). Overwintering mortality may be related to severe winter conditions or predation. Siuda (1963) reported that the spider *Tegenaria domestica* preys on overwintering females of *E. tenax*. Certainly, dead hoverflies are often found entangled in spider webs in hibernacula (Bressin 1999). As little is known about the exact mortality rates during hibernation, this mortality would be an calibrated parameter in the model.

Mortalities will also be associated with management events. We hypothesise that if *E. tenax* eggs or larvae are present in the field, particularly within slurry deposits, at the time of soil cultivation, their probability of survival is minimal. Consequently, we assume 100% mortality for these stages during cultivation events. This assumption is based on the mechanical disruption of the soil structure by most cultivation methods, including light harrowing, which typically penetrates to depths of 2–5 cm, and the disturbance of technological lines by heavy machinery, where slurry tends to accumulate and larval development may occur. We do not expect *E. tenax* eggs or larvae to be present in the field during harvest, as these stages are associated with liquid environments. Therefore, mortality due to harvest operations is considered negligible. For pupae which use dry land, mortality values for soil cultivation can be parameterised using data for the ground beetle *Bembidion lampros* (Thorbek and Bilde 2004), and incorporated into the model for sensitivity testing. We do not expect *E. tenax* pupae to be present in the field during harvest. Other managements could be considered on a case-by-case basis as needed when applying the model. The potential impacts of various agricultural practices on *E. tenax* population dynamics can be evaluated using the model, and sensitivity analyses can be conducted to assess the robustness of these assumptions.

Finally, we assume that the mortality of non-diapause stages will occur with the onset of winter (here, we assume December 1st) or with negative temperatures lower than a minimum temperature threshold (*MinT*), initially assumed to be -10 °C.

Discussion

The *E. tenax* model is based on a relatively large body of literature; however, many processes have uncertain parameter values and/or mechanisms. Information comes primarily from laboratory studies and, in some cases, from other hoverfly species. Thus, some crucial information about the species is still missing or uncertain.

The available data were insufficient to estimate the thermal performance curves for all developmental stages of *E. tenax*. Only the pupa stage had enough data relating developmental time with temperature, but the temperature range tested was narrow and did not exceed 26 °C. This limitation likely biased the fitting of the thermal performance curves and the determination of thermal optima and maxima for the pupa development. Indeed, the thermal performance curve model of the Lobry–Rosso–Flandrois predicted a thermal optimum of 26 °C, the highest temperature for which pupa development data were available. In addition, the primary aim of the collected studies relating developmental time with temperature was not to investigate the effect of temperature variation on development or to determine optimal thermal conditions. Instead, these studies often focused on the effects of diet or population density on development (with the goal of finding the optimal conditions for rearing *E. tenax* in the laboratory). They thus were typically conducted at a single temperature or over a limited temperature range; similarly, studies examining the impact of temperature on phenotypic variation tested only a narrow range of temperatures. Thus, the effects of temperature on egg and larval development were explained by a quadratic relationship. For both the egg and larval stages, the thermal minimums and maximums for development need to be calibrated. Due to the brief duration of the egg stage (typically 1–4 days), the impact of limited empirical data on the accuracy of phenological predictions for this stage is anticipated to be minimal. In contrast, the larval stage is longer and more sensitive to environmental variability; therefore, uncertainties in thermal parameters may affect the predicted duration of larval development more significantly.

The available data on the survival of juvenile stages, particularly for the egg and larva, is limited. A thermal performance curve linking survival and temperature could only be fitted for the pupa stage. However, the fit was suboptimal due to the narrow range of temperatures tested and the availability of multiple measurements only at selected temperatures, which were associated with treatments involving stable temperatures but varying other conditions.

Unfortunately, there is limited data available regarding the diet of adult hoverflies in relation to different behaviours. According to Gilbert (1985b), who categorised hoverflies based on their dietary preferences, *E. tenax* feeds on both pollen and nectar, with females consuming more pollen than nectar. However, this study did not link dietary preferences with hoverfly behaviour. Therefore, we hypothesise that the dietary preferences of female *E. tenax* will follow the pattern observed in *R. campestris* (Haslett 1989), where the switch between pollen and nectar preferences was related to the degree of ovarian development in females. In our model, the behaviour of female *E. tenax* is driven by "reproductive goals," which set the daily "foraging goals," i.e., the proportions of pollen to nectar in a daily diet. During ovarian development and egg maturation, females will primarily feed on pollen, while during mating and oviposition, they will mainly feed on nectar. We propose to initially set the proportions of

pollen to nectar linked to these behaviours based on the study of gut content in *R. campestris* (Haslett 1989). However, these proportions could be adjusted during the calibration process or as new data for the species become available. Furthermore, the relationship between nutrient intake and the development of ovaries and egg maturation is not fully understood. We do not know the exact amount of pollen or proteins required to mature a certain number of eggs. Thus, in the first version of the model, we assume that all pollen from preferred plants provides the same amount of nutrients and is equally beneficial. The same assumption applies to nectar, as there is no information on nectar preferences in *E. tenax*. In addition, we propose to track separately the amount of nutrients needed for ovary development and egg maturation. Although this separation is artificial, it allows a consistent tracking mechanism for the gut content associated with each clutch produced by a female. It can also be applied regardless of the hoverfly"s generation.

In the initial version of the model, we do not plan to simulate the energetic budget of the hoverfly, which would link energy losses with flying and mating activities and energy gains with nectar foraging. Instead, the model will track the percentage of gut filling separately for pollen and nectar resources, according to the foraging goals. This simplified approach is necessitated by the limited data available on the energetic demands of hoverflies. Based on literature information (Gilbert 1983), we assume that the energy needed for flying and mating activities is easily regained even on low-rewarding plants, and if any nectar is available, it is enough for the females (the males consume mostly nectar, but we do not model males). Thus, females rely mainly on having enough pollen to ensure their eggs" maturation, which is tracked in the model.

The variability in *E. tenax* reproduction parameters can depend on various factors, including energy reserves, nutrient availability, and environmental conditions (Gladies 1994). However, the detailed mechanisms remain poorly understood. The reproduction parameters available for *E. tenax* were mostly measured under laboratory conditions, typically with stable food and temperature settings. Consequently, whether the same or greater variability exists under field conditions is unclear. Additionally, no studies have compared the reproduction parameters between the spring/summer and autumn generations. In the model, total potential fecundity is assumed to depend linearly on the mass of the female, following the general relationships described by Honěk (1993), but mechanisms included allow the actual fecundity to be reduced by a scarcity of floral resources and unfavourable environmental conditions.

While there are existing models of clutch size for insects, particularly in relation to optimal foraging theory (e.g., Skinner 1985; Wilson and Lessells 1994), none have been developed specifically for hoverflies, to our knowledge. These models consider factors such as a female"s ability to recognize the presence of existing clutches or eggs in a given larval habitat to avoid excessive competition among larvae or the ability to delay oviposition until better environmental conditions arise, thereby increasing the survival chances of their progeny. These mechanisms have not been investigated in saprophagous hoverflies. Therefore, we have made some assumptions that may be modified as new data for the species become available.

We assume that the availability of floral resources and environmental (weather) conditions significantly impact the clutch size and fecundity of female *E. tenax*. In the model, the probability of laying a larger clutch is assumed to

decrease over time. This assumption reflects the female"s decreasing willingness to continue feeding to gather more nutrients for egg maturation, aiming to reduce the risk of predation and increase the survival chances of the progeny. Additionally, we assume that if the clutch size is smaller than the maximum allowed, the remaining egg load is “lost.” This assumption is based on the phenomenon of egg resorption. Egg resorption is a mechanism known in many insects and allows energy conservation for maternal survival and future reproduction by facilitating the maturation of new oocytes (Rosenheim et al. 2000). Although not reported for saprophagous hoverflies, this mechanism exists in many aphidophagous hoverfly species, where the absence of aphids on host plants can lead to egg resorption by adult females (Schneider 1969; Branquart and Hemptinne 2000; Orengo-Green et al. 2022).

Developing the formal model for *E. tenax* presented two significant challenges linked with modelling of the availability and quality of larval habitats, and dispersal. In the model, the availability and quality of larval habitats, along with the availability of floral resources, are critical limiting factors that regulate population dynamics at the landscape level. Therefore, accurately assessing these factors is crucial for the model"s performance. Given the difficulty in mapping the exact locations of larval habitats at the landscape level due to their diversity and *E. tenax* adaptability to different environments, we propose characterizing each landscape element by a larval habitat quality index. This index is linked to larval density estimates obtained from field data and influences the attractiveness of a patch in the female"s oviposition selection process. The proposed index is based on a general classification of landscape elements according to their suitability as habitats for *Eristalis* larvae, derived from literature, and an assessment of moisture conditions influenced by soil properties, local topography, and current meteorological conditions. We assume that potential larval microhabitats may vary in abundance within the same habitat type (e.g., wet grassland) depending on actual wetness conditions, which fluctuate over time. This mechanism produces a pattern of maximum possible larval densities that changes over space and time, allowing for the introduction of year-to-year variation in *E. tenax* population dynamics, observable in the field. The larval habitat quality index can be refined as more data become available, for example, by linking real larval densities with factors such as the chemical or nutritional characteristics of the rearing media.

The larval habitat quality values are scaled based on the minimum and maximum larval densities observed in the field. However, due to limited data on field larval densities, it was not feasible to adapt these minimum and maximum values for each habitat or landscape element type. *Eristalis* eggs are laid in clutches, resulting in a patchy distribution of larvae, which complicates obtaining accurate density measurements. Consequently, field measurements must be taken with care and cannot be directly extrapolated to represent densities for the entire habitat. This is particularly important as the model incorporates larval density-dependent mechanisms related to survival and growth, which are linked to adult mass.

Designing dispersal functions is challenging because they need to be integrated with foraging and oviposition behaviours. In our approach, daily behaviour is driven by reproductive goals, which are linked to foraging goals. The achievement of these goals depends on the spatial and temporal distribution of floral resources and is constrained by the movement capabilities of *E. tenax*.

During the calibration stage, it is essential to carefully evaluate the behaviours of *E. tenax*. This evaluation will focus on the parameters implemented in the hoverfly model and their interaction with the detailed patterns provided by the landscape model. The landscape model offers spatial and temporal patterns of resources, making it crucial for the level of detail in both model components to be aligned. This alignment ensures that emergent patterns accurately reflect the real-world dynamics of *E. tenax* populations.

Given the ecological significance of migration for *E. tenax*, we assume that females of the autumn generation may exhibit migratory behaviour with a certain probability. However, as the primary objective of the current model is to inform risk assessment, the probability of migration will be set to zero in the first version of the model. This simplification is intended to prevent the confounding and dilution of potential pesticide effects, thereby enabling clearer interpretation of local risk dynamics.

Overall, the *E. tenax* model proposed lacks some of the details characteristic for other ALMaSS models; nevertheless, it should provide a dynamic model that can respond to variations in weather, habitat configuration, and resource availability. Importantly, this formal model represents a foundational implementation that is intended to be refined through a post-deployment calibration phase. Calibration will be conducted using a pattern-oriented modelling (POM) approach, which employs multiple empirical patterns to iteratively guide model selection, structure, and parameterisation. Based on our prior experience with individual-based models for other beneficial insects, we have found POM to be particularly effective in addressing initial data limitations and enhancing both model realism and predictive capacity. The current formal model serves as a structured synthesis of available ecological and biological knowledge of the species, designed to support future refinement and application. Rather than offering a definitive representation, it provides a robust starting point for iterative development and validation. As such, it establishes a baseline framework against which pesticide-induced effects can be evaluated under carefully constructed scenario analyses.

Acknowledgements

We would like to thank Karin Nordström for kindly providing the raw data and Francis Gilbert for sharing the unpublished data and publications on *E. tenax*. We would also like to thank both reviewers for their valuable insights and constructive comments, which helped us to significantly improve the manuscript. This study was supported by the PollinERA project. PollinERA receives funding from the European Union"s Horizon Europe research and innovation Programme under grant agreement No.101135005. Views and opinions expressed are those of the author(s) only and do not necessarily reflect those of the European Union (EU) or the European Research Executive Agency (REA). Neither the EU nor REA can be held responsible for them.

Additional information

Conflict of interest

The authors have declared that no competing interests exist.

Ethical statement

No ethical statement was reported.

Use of AI

No use of AI was reported.

Funding

No funding was reported.

Author contributions

Conceptualization: EZ, AW, CJT. Formal analysis: EZ, AW. Funding acquisition: CJT. Investigation: AW, EZ. Supervision: CJT. Visualization: EZ. Writing - original draft: EZ. Writing - review and editing: AW, CJT.

Author ORCIDs

Elżbieta Ziółkowska https://orcid.org/0000-0002-7213-2200
Aleksandra Walczyńska https://orcid.org/0000-0002-0464-1855
Christopher John Topping https://orcid.org/0000-0003-0874-7603

Data availability

All of the data that support the findings of this study are available in the main text.

References

An L, Neimann A, Eberling E, Algora H, Brings S, Lunau K (2018) The yellow specialist: dronefly *Eristalis tenax* prefers different yellow colours for landing and proboscis extension. Journal of Experimental Biology 221: jeb184788. https://doi.org/10.1242/jeb.184788

App M, Hellwig N, Schneider-Hohenbrink A-K, Burmeister J, Schröder B, Thiele J (2025) SyrFitSources: An agent-based model to investigate the effects of land use on the population dynamics of aphidophagous hoverflies. Ecological Modelling 507: 111098. https://doi.org/10.1016/j.ecolmodel.2025.111098

Arrignon F, Deconchat M, Sarthou JP, Balent G, Monteil C (2007) Modelling the overwintering strategy of a beneficial insect in a heterogeneous landscape using a multi-agent system. Ecological Modelling 205: 423–436. https://doi.org/10.1016/j.ecolmodel.2007.03.006

Aubert J, Aubert JJ, Goeldlin de Tiefenau P (1976) Twelve years of systematic collecting of syrphids (Diptera) at the Bretolet pass (Alps of Valais). Mitteilungen der Schweizerischen Entomologischen Gesellschaft 49(1/2): 115–142.

Aubert J, Goeldlin P, Lyon JP (1969) Essais de marquage et de reprise d"insectes migrateurs en automne 1968. Mitteilungen der Schweizerischen Entomologischen Gesellschaft 42: 140–166.

Bailes EJ, Deutsch KR, Bagi J, Rondissone L, Brown MJF, Lewis OT (2018) First detection of bee viruses in hoverfly (syrphid) pollinators. Biology Letters 14: 20180001. https://doi.org/10.1098/rsbl.2018.0001

Basley K, Davenport B, Vogiatzis K, Goulson D (2018) Effects of chronic exposure to thiamethoxam on larvae of the hoverfly *Eristalis tenax* (Diptera, Syrphidae). PeerJ 6: e4258. https://doi.org/10.7717/peerj.4258

Branquart E, Hemptinne JL (2000) Development of ovaries, allometry of reproductive traits and fecundity of Episyrphus balteatus (Diptera: Syrphidae). European Journal of Entomology 97: 165–170. https://doi.org/10.14411/eje.2000.031

Bressin S (1999) Environmental physiology of two hoverflies, "*Eristalis tenax*" and E. pertinax". University of St Andrews, St Andrews.

Brown AD (2016) Looking Outward From The Village: The Contingencies Of Soil Moisture On The Prehistoric Farmed Landscape Near Goodman Point Pueblo. Master of Science (Applied Geography), 331 pp.

Buckton GB (1895) The natural history of *Eristalis tenax* or the drone-fly. Macmillan, London, New York.

Campan M (1968) Preliminary observations on the activity rhythm of female *Eristalis tenax* at the oviposition site: influence of meteorological factors [Observations preliminaires sur le rythme d"activité des femelles d"*Eristalis tenax* (Dipteres, Syrphides) aux lieux de ponte influence des facteurs meteorologiques]. Revue du comportement animal 3: 69–76.

Campan M (1973) Study of seasonal variations in the frequency of visits to laying sites by females of *Eristalis tenax* (Diptera, Syrphidae) [Étude des variations saisonnières du rythme de fréquentation des lieux de ponte chez les femelles d"*Eristalis tenax* (Diptères, Syrphides).]. Bulletin de la Société d"histoire naturelle de Toulouse 109: 119–130.

Campan M, Campan R (1979) The timing of the selection of the egg-laying site, in relation to olfactive and visual stimulus, in the *Eristalis tenax* (Diptera, Syrphides) [Déroulement temporel, chez les femelles d"*Eristalis tenax* (Diptères, Syrphides), de l"approche du lieu de ponte, en relation avec des stimulus olfactifs et visuels]. Biology of Behaviour 1: 43–60.

Campoy A, Egea-Casas O, Pérez-Bañón C, Rojo S (2022) Effect of cold storage on the pupal development of two pollinators, *Eristalinus aeneus* and *Eristalis tenax*. Entomologia Experimentalis et Applicata 170: 110–121. https://doi.org/10.1111/eea.13117

Campoy A, Pérez-Bañón C, Rojo S (2020) Intra-puparial development in the hoverflies *Eristalinus aeneus* and *Eristalis tenax* (Diptera: Syrphidae). Journal of Morphology 281: 1436–1445. https://doi.org/10.1002/jmor.21257

Cao L, Zeng Q, Ren Q, Zeng A, Zhang Y (2022) Morphological characteristics and biological cycle of the hoverfly Eristalinus arvorum (Fabricius, 1787) (Diptera, Syrphidae). Frontiers in Sustainable Food Systems 6: 1052908. https://doi.org/10.3389/fsufs.2022.1052908

Čičková H, Newton GL, Lacy RC, Kozánek M (2015) The use of fly larvae for organic waste treatment. Waste Management 35: 68–80. https://doi.org/10.1016/j.wasman.2014.09.026

Collett TS, Land MF (1978) How hoverflies compute interception courses. Journal of Comparative Physiology 125: 191–204. https://doi.org/10.1007/BF00656597

Conn DLT (1976) Estimates of population size and longevity of adult narcissus bulb fly Merodon equestris Fab. (Diptera: Syrphidae). Journal of Applied Ecology 13: 429–434. https://doi.org/10.2307/2401792

Cowgill SE (1991) The foraging ecology of hoverflies (Diptera:Syrphidae) and the potential for manipulating their distribution on farmland. University of Southampton, Doctoral Thesis. https://eprints.soton.ac.uk/460469/

Daňková K, Nicholas S, Nordström K (2023) Temperature during pupal development affects hoverfly developmental time, adult life span, and wing length. Ecology and Evolution 13: e10516. https://doi.org/10.1002/ece3.10516

Davenport J (1992) Animal life at low temperature. Chapman & Hall. London. https://doi.org/10.1007/978-94-011-2344-0

de Melo MLA, Inforsato L, Pinheiro EAR, de Jong van Lier Q (2023) Plant available water predicted by a flux-based approach. Geoderma 429: 116253. https://doi.org/10.1016/j.geoderma.2022.116253

Dolley WL, Hassett CC, Bowen WB, Phillies G (1933) Culture of the drone fly, *Eristalis tenax*. Science 78: 313–314. https://doi.org/10.1126/science.78.2023.313

Doyle T, Hawkes WLS, Massy R, Powney GD, Menz MHM, Wotton KR (2020) Pollination by hoverflies in the Anthropocene. Proceedings of the Royal Society B 287: 20200508. http://doi.org/10.1098/rspb.2020.0508

Duan X, Wallis D, Hatjina F, Simon-Delso N, Bruun Jensen A, Topping CJ (2022) ApisRAM Formal Model Description. EFSA Supporting Publications 19: 7184E. https://doi.org/10.2903/sp.efsa.2022.EN-7184

Francuski L, Milankov V (2015) Assessing spatial population structure and heterogeneity in the dronefly. Journal of Zoology 297: 286–300. https://doi.org/10.1111/jzo.12278

Francuski L, Djurakic M, Ståhls G, Milankov V (2014) Landscape genetics and wing morphometrics show a lack of structuring across island and coastal populations of the drone fly in the Mediterranean. Journal of Zoology 292: 156–169. https://doi.org/10.1111/jzo.12090

Francuski L, Ludoški J, Milankov V (2013a) Phenotypic diversity and landcape genetics of *Eristalis tenax* in a spatially heterogeneous environment, Durmitor Mountain (Montenegro). Annales Zoologici Fennici 50: 262–278. https://doi.org/10.5735/085.050.0502

Francuski L, Djurakic M, Ludoški J, Milankov V (2013b) Landscape genetics and spatial pattern of phenotypic variation of *Eristalis tenax* across Europe. Journal of Zoological Systematics and Evolutionary Research 51: 227–238. https://doi.org/10.1111/jzs.12017

Gatter W (1976) Der Zug der Schwebfliegen nach planmäßigen Fängen am Randecker Maar (Schwäbische Alb) (Dip. Syrphidae). Atalanta 7: 4–18.

Gatter W, Ebenhöh H, Kima R, Gatter W, Scherer F (2020) 50-jährige Untersuchungen an migrierenden Schwebfliegen, Waffenfliegen und Schlupfwespen belegen extreme Rückgänge (Diptera: Syrphidae, Stratiomyidae; Hymenoptera: Ichneumonidae). Entomologische Zeitschrift 130(3): 131–142.

Gatter W, Schmid U, Gatter W, Jauch G (1990) Die Wanderungen der Schwebfliegen (Diptera, Syrphidae) am Randecker Maar. Zoologische Staatssammlung München, Supplement 15: 1e100.

Gilbert FS (1981) Morphology and the foraging ecology of hoverflies (Diptera: Syrphidae). Ph.D. thesis, Cambridge University.

Gilbert FS (1983) The foraging ecology of hoverflies (Diptera, Syrphidae): circular movements on composite flowers. Behavioral Ecology and Sociobiology 13: 253–257. https://doi.org/10.1007/BF00299672

Gilbert FS (1985a) Diurnal activity patterns in hoverflies (Diptera, Syrphidae). Ecological Entomology, 10: 385–392. https://doi.org/10.1111/j.1365-2311.1985.tb00736.x

Gilbert FS (1985b) Ecomorphological relationships in hoverflies (Diptera, Syrphidae). Proceedings of the Royal Society B 224: 91–105. https://doi.org/10.1098/rspb.1985.0023

Gilbert FS (1986) Hoverflies. Naturalist" Handbook. Cambridge University Press, Cambridge.

Gladis T (1993) Laboratory Rearing of Some *Eristalines* (Diptera, Syrphidae) and the Possibility of their Use in Plant Cultures [Laborzucht einiger Eristalinen (Diptera,

Syrphidae) und Möglichkeiten für ihren Einsatz in der Pflanzenzüchtung]. Verhandlungen der Westdeutscher Entomologentag, Düsseldof, 139–152.

Gladis T (1994a) Establishment and utilization of a mass rearing of *Eristalis tenax* (Diptera, Syrphidae) in the Gatersleben gene-bank. Insecta 1: 287–294.

Gladis T (1994b) Rearing methods and beneficial likelihood for native insects as pollinators of outcrossing cultivated plant species [Zuchtmethoden und Nutzungsmöglichkelten für einheimische Insekten als Bestäuber allogamer kulturpflanzenarten]. Schriftenreihe des Länderinstituts für Bienenkunde (ed. by C Hedtke), Länderinstitut für Bienenkunde, Hohen Neuendorf, Germany, 10–23.

Gleiser RM, Urrutia J, Gorla DE (2000) Body size variation of the floodwater mosquito Aedes albifasciatus in Central Argentina. Medical and Veterinary Entomology 14: 38–43. https://doi.org/10.1046/j.1365-2915.2000.00217.x

Golding YC, Edmunds M (2000) Behavioural mimicry of honeybees (Apis mellifera) by droneflies (Diptera: Syrphidae: *Eristalis* spp.). Proceedings of the National Academy of Science of India B 267: 903–909. https://doi.org/10.1098/rspb.2000.1088

Grimm V, Railsback SF (2005) Individual-based Modeling and Ecology. Princeton University Press, Princeton and Oxford, 448 pp. https://doi.org/10.1515/9781400850624

Halloway BA (1976) Pollen-feeding in hover-flies (Diptera: Syrphidae). New Zealand Journal of Zoology 3: 339–350. https://doi.org/10.1080/03014223.1976.9517924

Harris-Cypher A, Roman C, Higgins G, Scheufele S, Legrand A, Wallingford A, Sideman RG (2023) A field survey of syrphid species and adult densities on annual flowering plants in the Northeastern United States. Environmental Entomology 52: 175–182. https://doi.org/10.1093/ee/nvad016

Hartley JC (1961) A taxonomic account of the larvae of some British syrphidae. Proceedings of the Zoological Society of London 136: 505–573. https://doi.org/10.1111/j.1469-7998.1961.tb05891.x

Haslett JR (1989) Adult feeding by holometabolous insects: pollen and nectar as complementary nutrient sources for Rhingia campestris (Diptera: Syrphidae). Oecologia 81: 361–363. https://doi.org/10.1007/BF00377084

Hawkes WLS, Walliker E, Gao B, Forster O, Lacey K, Doyle T, Massy R, Roberts NW, Reynolds DR, Özden Ö, Chapman JW, Wottonet KR (2022) Huge spring migrations of insects from the Middle East to Europe: quantifying the migratory assemblage and ecosystem services. Ecography 10: e06288. https://doi.org/10.1111/ecog.06288

Heal J (1979) Colour patterns of Syrphidae: I. Genetic variation in the dronefly *Eristalis tenax*. Heredity 42: 223–236. https://doi.org/10.1038/hdy.1979.24

Heal J (1982) Colour patterns of syrphidae: IV. Mimicry and variation in natural populations of *Eristalis tenax*. Heredity 49: 95–109. https://doi.org/10.1038/hdy.1982.68

Heal JR (1989) Variation and seasonal changes in hoverfly species: interactions between temperature, age and genotype. Biological Journal of the Linnean Society 36: 251–269. https://doi.org/10.1111/j.1095-8312.1989.tb00493.x

Hlaváček A, Lučan RK, Hadrava J (2022) Autumnal migration patterns of hoverflies (Diptera: Syrphidae): interannual variability in timing and sex ratio. PeerJ 10: e14393. https://doi.org/10.7717/peerj.14393

Hoffmann F (2005) Biodiversity and pollination: Flowering plants and flower-visiting insects in agricultural and semi-natural landscapes. Rijksuniversiteit Groningen, 225 pp.

Holloway BA (1976) Pollen-feeding in hover-flies (Diptera: Syrphidae). New Zealand Journal of Zoology 3: 339–350. https://doi.org/10.1080/03014223.1976.9517924

Honěk A (1993) Intraspecific Variation in Body Size and Fecundity in Insects: A General Relationship. Oikos 66: 483–492. https://doi.org/10.2307/3544943

Hondelmann P, Poehling H-M (2007) Diapause and overwintering of the hoverfly *Episyrphus balteatus*. Entomologia Experimentalis et Applicata 124: 189–200. https://doi.org/10.1111/j.1570-7458.2007.00568.x

Howlett BG, Gee M (2019) The potential management of the drone fly (*Eristalis tenax*) as a crop pollinator in New Zealand. New Zealand Plant Protection 72: 221–229. https://doi.org/10.30843/nzpp.2019.72.304

Howlett BG, Butler RC, Nelson WR, Donovan BJ (2013) Impact of climate change on crop pollinator activity in New Zealand. Ministry for Primary Industries, Wellington, New Zealand.

Hurtado P (2013) Intra-puparial development in the hoverflies Eristalinus aeneus and *Eristalis tenax* (Diptera: Syrphidae). University of Alicante, Alicante, Spain.

Ibrahim IA (1976) Studies on certain myiatic insects. MSc Thesis, Department of Entomology, Ain Shams University, Cairo, 96 pp.

Irvin NA, Wratten SD, Frampton CM, Bowie MH, Evans AM, Moar NT (1999) The phenology and pollen feeding of three hover fly (Diptera: Syrphidae) species in Canterbury, New Zealand. New Zealand Journal of Zoology 26: 105–115. https://doi.org/10.1080/03014223.1999.9518182

Iwasa Y, Suzuki Y, Matsuda H (1984) Theory of oviposition strategy of parasitoids. I. Effect of mortality and limited egg number. Theoretical Population Biology 26: 205–227. https://doi.org/10.1016/0040-5809(84)90030-3

Jarlan A, De Oliveira D, Gingras J (1997) Effects on *Eristalis tenax* (Diptera: Syrphidae) pollination on characteristics of greenhouse green pepper fruits. Journal of Economic Ecology 90: 1650–1654. https://doi.org/10.1093/jee/90.6.1650

Jensen ME, Haise HR (1963) Estimating Evapotranspiration from Solar Radiation. Journal of the Irrigation and Drainage Division 89: 15–41. https://doi.org/10.1061/JRCEA4.0000287

Kamdem MM, Otomo PV (2023) Developmental performance of *Eristalis tenax* larvae (Diptera: Syrphidae): Influence of growth media and yeast addition during captive rearing. Journal of Experimental Zoology A 339: 503–513. https://doi.org/10.1002/jez.2696

Kamdem MM, Sithole S, otomo PY (2024) Effects of imidacloprid on the survival and biomarker responses of *Eristalis tenax* larvae (Diptera: Syrphidae): a comparative study between indoor and outdoor exposures. Journal of Environmental Science and Health, Part B 59(6): 333–340. https://doi.org/10.1080/03601234.2024.2343598

Kato M (1943) Ecological notes on the activities of some insects coming to the flowers of "Yatude", Fatsia japonica, with special reference to the ecological importance of the solar radiant energy. Scientific Reports Tohoku University Series IV 17: 255–262.

Kendall DA, Stradling DJ (1972) Some observation on overwintering of the drone fly, *Eristalis tenax* (L.) (Syrphidae). The Entomologist, 229–230.

Kikuchi T (1965) Studies on the coaction among insects visiting flowers VII. Diurnal rhythm of the appearance of the subordinate syrphid fly in relation to the presence of the dominant one. Science Reports of the Tohoku University IV 31: 207–215.

Klecka J, Hadrava J, Biella P, Akter A (2018) Flower visitation by hoverflies (Diptera: Syrphidae) in a temperate plantpollinator network. PeerJ 6: e6025. https://doi.org/10.7717/peerj.6025

Kobayashi M (1979) A study on multiplication and utilization of insects pollinating horticultural crops. Bulletin of the Iwate Horticultural Experiment Station Special Issue 1: 1–167.

Kolss M, Vijendravarma RK, Schwaller G, Kawecki TJ (2009) Life-history consequences of adaptation to larval nutritional stress in Drosophila. Evolution 63: 2389–2401. https://doi.org/10.1111/j.1558-5646.2009.00718.x

Krčmar S, Kučinić M, Durbešić P, Benović A (2010) Insects from the middle of the Adriatic sea. Entomologia Croatica 14: 75–84.

Lobry J, Rosso L, Flandrois JP (1991) A FORTRAN subroutine for the determination of parameter confidence limits in non-linear models. Binary 3: 25.

Lucas A, Bodger O, Brosi BJ, Ford CR, Forman DW, Greig C, Hegarty M, Neyland PJ, de Vere N (2018) Generalisation and specialisation in hoverfly (Syrphidae) grassland pollen transport networks revealed by DNA metabarcoding. Journal of Animal Ecology 87: 1008–1021. https://doi.org/10.1111/1365-2656.12828

Ludoški J, Francuski L, Gojković N, Matić B (2023) Sexual size and shape dimorphism, and allometric scaling in the pupal and adult traits of *Eristalis tenax*. Ecology and Evolution 13: e9907. https://doi.org/10.1002/ece3.9907

Lunau K, Wacht S (1994) Optical releasers of the innate proboscis extension in the hoverfly *Eristalis tenax* L. (Syrphidae, Diptera). Journal of Comparative Physiology A 174: 575–579. https://doi.org/10.1007/BF00217378

Lunau K, Wacht S (1997) Innate flower recognition in the hoverfly *Eristalis tenax* L. Mitteilungen der Deutschen Gesellschaft für Allgemeine und Angewandte Entomologie 11: 481–484.

Mahmoud MAM (1997) Ecological and microbiological studies on syrphid larvae inhabiting sewage water. MSc Thesis, Faculty of Science, Suez Canal University, Egypt, 149 pp.

Martins CAH, Azpiazu C, Bosch J, Burgio G, Dindo ML, Francati S, Sommaggio D, Sgolastra F. (2024) Different Sensitivity of Flower-Visiting Diptera to a Neonicotinoid Insecticide: Expanding the Base for a Multiple-Species Risk Assessment Approach. Insects 15(5): 317. https://doi.org/10.3390/insects15050317

Matoušková E, Štenc J, Janovský Z (2023) Innate preferences of *Eristalis tenax* L. (Syrphidae) for flower colour, size and symmetry are more intricate than the simple additive model. Biological Journal of the Linnean Society 140: 110–119. https://doi.org/10.1093/biolinnean/blad035

McKee TB, Doesken NJ, Kleist J (1993) The relationship of drought frequency and duration to time scales. In Propeedings of the 8th Conference on Applied Climatology, Anaheim, CA, USA, 179–184.

Moog O, Ernst C (1978) Die Schwebfliege Eristalomyia tenax (L.) - ein Wintergast in Hohlen (Diptera: Syrphidae). Hohle 29: 15–7.

Nagloo N, Rigosi E, O"Carroll DC (2023) Acute and chronic toxicity of imidacloprid in the pollinator fly, *Eristalis tenax* L., assessed using a novel oral bioassay. Ecotoxicology and Environmental Safety 251: 114505. https://doi.org/10.1016/j.ecoenv.2023.114505

Nicholas S, Thyselius M, Holden M, Nordström K (2018) Rearing and long-term maintenance of *Eristalis tenax* hoverflies for research studies. Journal of Visualized Experiments 135: e57711. https://doi.org/10.3791/57711-v

Nikolaou G, Neocleous D, Manes A, Kitta E (2024) Calibration and validation of solar radiation-based equations to estimate crop evapotranspiration in a semi-arid climate. International Journal of Biometeorology 68: 1–15. https://doi.org/10.1007/s00484-023-02566-5

Orengo-Green JJ, Casas JL, Marcos-García MA (2022) Effect of abiotic climatic factors on the gonadal maturation of the biocontrol agent Sphaerophoria rueppellii (Wiedemann, 1830) (Diptera: Syrphidae). Insects 13: 573. https://doi.org/10.3390/insects13070573

Ottenheim MM, Volmer AD, Holloway GJ (1996) The genetics of phenotypic plasticity in adult abdominal colour pattern of *Eristalis arbustorum*. Heredity 77: 493–499. https://doi.org/10.1038/hdy.1996.176

Ouvrard P, Transon J, Jacquemart AL (2018) Flower-strip agri-environment schemes provide diverse and valuable summer flower resources for pollinating insects. Biodiversity and Conservation 27: 2193–2216. https://doi.org/10.1007/s10531-018-1531-0

Padfield D, O"Sullivan H, Windram F (2024) rTPC: Fitting and Analysing Thermal Performance Curves. R package version 1.0.7. https://doi.org/10.32614/CRAN.package.rTPC

Padfield D, O"Sullivn H, Pawar S (2021) rTPC and nls.multstart: A new pipeline to fit thermal performance curves in r. Methods in Ecology and Evolution 12: 1138–1143. https://doi.org/10.1111/2041-210X.13585

Parry HR, Bithell M (2011) Large Scale Agent-Based Modelling: A Review and Guidelines for Model Scaling. In: Heppenstall A, Crooks A, See L, Batty M (Eds) Agent-Based Models of Geographical Systems. Springer, Dordrecht. https://doi.org/10.1007/978-90-481-8927-4_14

Pérez-Bañón C, Hurtado P, García-Gras E, Rojo S (2013) SEM Studies on Immature Stages of the Drone Flies (Diptera, Syrphidae): *Eristalis similis* (Fallen, 1817) and *Eristalis tenax* (Linnaeus, 1758). Microscopy Research and Technique 76: 853–861. https://doi.org/10.1002/jemt.22239

Pinheiro LA, Torres LM, Raimundo J, Santos SAP (2015) Effects of pollen, sugars and honeydew on lifespan and nutrient levels of Episyrphus balteatus. BioControl 60: 47–57. https://doi.org/10.1007/s10526-014-9621-8

Plume L, Maestracci PY, Gibernau M (2024) Insight into the diversity of flower-visiting hoverflies (Diptera: Syrphidae) in shrubland Maquis Around Ajaccio (South-West Corsica, France). Journal of Applied Entomology. https://doi.org/10.1111/jen.13379

Ratkowsky DA, Reddy GVP (2017) Empirical model with excellent statistical properties for describing temperature-dependent developmental rates of insects and mites. Annals of the Entomological Society of America 110: 302–309. https://doi.org/10.1093/aesa/saw098

Ratkowsky DA, Lowry RK, McMeekin TA, Stokes AN, Chandler RE (1983) Model for bacterial growth rate throughout the entire biokinetic temperature range. Journal of Bacteriology 154: 1222–1226. https://doi.org/10.1128/jb.154.3.1222-1226.1983

Reemer M, Renema W, van Steenis W, Zeegers Th, Barendregt A, Smit JT, van Veen MP, van Steenis J, van der Leij LJJM (2009) De Nederlandse zweefvliegen (Diptera: Syrphidae). – Nederlandse Fauna. Leiden. Nationaal Natuurhistorisch Museum Naturalis, Uitgeverij, European Invertebrate Survey – Nederland.

Reynolds SK, Clem CS, Fitz-Gerald B, Young AD (2024) A comprehensive review of long-distance hover fly migration (Diptera: Syrphidae). Ecological Entomology 49: 749–767. https://doi.org/10.1111/een.13373

Rigosi E, O"Carroll (2021) Acute Application of Imidacloprid Alters the Sensitivity of Direction Selective Motion Detecting Neurons in an Insect Pollinator. Frontiers in Physiology 12: 682489. https://doi.org/10.3389/fphys.2021.682489

Rosenheim JA, Heimpel GE, Mangel M (2000) Egg maturation, egg resorption and the costliness of transient egg limitation in insects. Proceedings of the Royal Society B. Biological Sciences 267: 1565–1573. https://doi.org/10.1098/rspb.2000.1179

Rosso L, Lobry JR, Flandrois JP (1993) An unexpected correlation between cardinal temperatures of microbial growth highlighted by a new model. Journal of Theoretical Biology 162: 447–463. https://doi.org/10.1006/jtbi.1993.1099

Rotheray GE (1993) Colour guide to hoverfly larvae (Diptera, Syrphidae) in Britain and Europe. Dipterists Digest 9: 156.

Schneider F (1969) Bionomics and physiology of aphidophagous Syrphidae. Annual Reviews of Entomology 14: 103–124. https://doi.org/10.1146/annurev.en.14.010169.000535

Scott SM, Barlow CA (1984) Effect of prey availability during development on the reproductive output of Metasyrphus corollae (Diptera: Syrphidae). Environmental Entomology 13: 669–674. https://doi.org/10.1093/ee/13.3.669

Sengupta J, Naskar A, Maity A, Hazra S, Mukhopadhyay E, Banerjee D, Ghosh S (2016) An updated distributional account of Indian hover flies (Insecta: Diptera: Syrphidae) Journal of Entomological and Zoological Studies 4: 381–396.

Siuda K (1963) Ecological and ethological observations on *Eristalis tenax* (L.) (Diptera, fam. Syrphidae) and Tegenaria domestica Clerck (Arachnidae, fam. Agelenidae) hibernating in the caves and subterranean casemates in the vicinity of Cracow. Prace Zoologiczne 8: 83–112.

Skinner SW (1985) Clutch size as an optimal foraging problem for insects. Behavioral Ecology and Sociobiology 17: 231–238. https://doi.org/10.1007/BF00300141

Sotavalta O, Laulajainen E (1961) On the sugar consumption of the drone fly (*Eristalis tenax* L.) in flight experiments. Annales Academiae Scientiarum Fennicae Series A IV. Biologica, 53 pp.

Speight MCD (2018) Species accounts of European Syrphidae, Dublin.

Stearns SC (1992) The evolution of life histories. Oxford University Press, Oxford

Thorbek P, Bilde T (2004) Reduced numbers of generalist arthropod predators after crop management. Journal of Applied Ecology 41: 526–538. https://doi.org/10.1111/j.0021-8901.2004.00913.x

Thyselius M (2022) A behavioural investigation into *Eristalis tenax*. Pursuit, approach estimation, locomotor activity and rearing. PhD. University of Uppsala, ACTA UNIVERSITATIS UPSALIENSIS.

Thyselius M, Nordström K (2016) Hoverfly locomotor activity is resilient to external influence and intrinsic factors. Journal of Comparative Physiology A 202: 45–54. https://doi.org/10.1007/s00359-015-1051-2

Tomlison S, Menz MHM (2015) Does metabolic rate and evaporative water loss reflect differences in migratory strategy in sexually dimorphic hoverflies? Comparative Biochemistry and Physiology Part A: Molecular & Integrative Physiology 190: 61–67. https://doi.org/10.1016/j.cbpa.2015.09.004

Topping CJ, Alrøe HF, Farrell KN, Grimm V (2015) Per Aspera ad Astra: Through Complex Population Modeling to Predictive Theory. The American Naturalist 186: 669–674. https://doi.org/10.1086/683181

Topping C, Dalby L, Skov F (2016) Landscape structure and management alter the outcome of a pesticide ERA: Evaluating impacts of endocrine disruption using the ALMaSS European Brown Hare model. Science of The Total Environment 541: 1477–1488. https://doi.org/10.1016/j.scitotenv.2015.10.042

Topping CJ (2022) The Animal Landscape and Man Simulation System (ALMaSS): a history, design, and philosophy. Research Ideas and Outcomes 8. https://doi.org/10.3897/rio.8.e89919

Topping CJ, Duan X (2024a) ALMaSS Landscape and Farming Simulation: software classes and methods. Food and Ecological Systems Modelling Journal 5: e121215. https://doi.org/10.3897/fmj.5.121215

Topping CJ, Duan X (2024b) Managing large and complex population operations with agent-based models: The ALMaSS Population_Manager. Food and Ecological Systems Modelling Journal 5: e117593. https://doi.org/10.3897/fmj.5.117593

Topping CJ, Duan X (2025) The Formal Model for the butterfly Pieris napi (Lepidoptera, Pieridae) agent-based model in the Animal Landscape and Man Simulation System

(ALMaSS). Food and Ecological Systems Modelling Journal 6: e142802. https://doi.org/10.3897/fmj.6.142802

Topping CJ, Hansen TS, Jensen TS, Jepsen JU, Nikolajsen F, Odderskaer P (2003) ALMaSS, an agent-based model for animals in temperate European landscapes. Ecological Modelling 167: 65–82. https://doi.org/10.1016/S0304-3800(03)00173-X

Topping CJ, Kondrup Marcussen L, Thomsen P, Chetcuti J (2022) The Formal Model article format: justifying modelling intent and a critical review of data foundations through publication. Food and Ecological Systems Modelling Journal 3: e91024. https://doi.org/10.3897/fmj.3.91024

Upchurch A, Spurr CJ, Quarrell SR, Rowbottom RM, Allen GR (2023) Toward optimising reproductive output of *Eristalis tenax* (Diptera: Syrphidae) for commercial mass rearing systems. Austral Entomology 62: 360–371. https://doi.org/10.1111/aen.12660

van Huis A (2013) Potential of insects as food and feed in assuring food security. Annual Review of Entomology 58: 563–583. https://doi.org/10.1146/annurev-ento-120811-153704

Villa M, Santos SAP, López-Sáez JA, Pinheiro L, Marrão R, Aguiar C, Pereira JA (2021) Pollen feeding by syrphids varies across seasons in a Mediterranean landscape dominated by the olive orchard. Biological Control 156: 104556. https://doi.org/10.1016/j.biocontrol.2021.104556

Wacht S, Lunau K, Hansen K (1996) Optical and chemical stimuli control pollen feeding in the hoverfly *Eristalis tenax*. Entomologia Experimentalis et Applicata 80: 50–53. https://doi.org/10.1111/j.1570-7458.1996.tb00884.x

Wellington WG, Fitzpatrick SM (1981) Territoriality in the drone fly, *Eristalis tenax* (Diptera: Syrphidae). The Canadian Entomologist 113: 695–704. https://doi.org/10.4039/Ent113695-8

Willmer P (2011) Pollination and floral ecology. Princeton University Press, Princeton. https://doi.org/10.23943/princeton/9780691128610.001.0001

Wilson DJ, Gerard PJ, de Villiers JE (2009) Preventing rat-tailed maggot incursion into dairy sheds. New Zealand Plant Protection 62: 99–102. https://doi.org/10.30843/nzpp.2009.62.4792

Wilson K, Lessells CM (1994) Evolution of clutch size in insects. I. A review of static optimality models. Journal of Evolutionary Biology 7: 339–363. https://doi.org/10.1046/j.1420-9101.1994.7030339.x

Wotton KR, Gao B, Menz MHM, Morris RKA, Ball SG, Lim KS, Reynolds DR, Hu G, Chapman JW (2019) Mass seasonal migrations of hoverflies provide extensive pollination and crop protection services. Current Biology 29: 2167–2173. https://doi.org/10.1016/j.cub.2019.05.036

Wratten SD, Bowie MH, Hickman JM, Evans AM, Sedcole JR, Tylianakis JM (2003) Field boundaries as barriers to movement of hover flies (Diptera: Syrphidae) in cultivated land. Oecologia 134: 605–611. https://doi.org/10.1007/s00442-002-1128-9

Ziółkowska E, Jachuła J, Filipiak Z, Walczyńska A, Mikołajczyk Ł, Sowa G, Filipiak M (in preparation) A framework for calculating daily nectar, sugar and pollen production by different ecosystems, changing landscapes and phenologically shifting floras.

Ziółkowska E, Bednarska AJ, Laskowski R, Topping CJ (2023) The Formal Model for the solitary bee Osmia bicornis L. agent-based model. Food and Ecological Systems Modelling Journal 4: e102102. https://doi.org/10.3897/fmj.4.102102